Branched-Chain Amino Acid Metabolism is Regulated by ERRα and is Further Impaired by Glucose Loading in Type 2 Diabetes

Rasmus J.O. Sjögren[1*], David Rizo-Roca[1*], Alexander V. Chibalin[1], Elin Chorell[2], Regula Furrer[3], Shintaro Katayama[4], Jun Harada[5], Håkan K.R. Karlsson[1], Christoph Handschin[3], Thomas Moritz[6], Anna Krook[7], Erik Näslund[8], and Juleen R. Zierath[1,7]

[1]Department of Molecular Medicine and Surgery, Integrative Physiology, Karolinska Institutet, Stockholm, 171 77, Sweden.

[2]Department of Public Health and Clinical Medicine, Umeå University, Umeå, 901 87, Sweden.

[3]Biozentrum, University of Basel, Basel, 4056, Switzerland.

[4]Department of Biosciences and Nutrition, Karolinska Institutet, Huddinge, 141 83, Sweden.

[5]Cardiovascular-Metabolics Research Laboratories, Daiichi Sankyo Co., Ltd., Tokyo, Japan.

[6]Swedish Metabolomics Centre, Department of Forest Genetics and Plant Physiology, Swedish University of Agricultural Sciences, Umeå 750 07, Sweden.

[7]Department of Physiology and Pharmacology, Integrative Physiology, Karolinska Institutet, Stockholm, 171 77, Sweden.

[8]Division of Surgery, Department of Clinical Sciences, Danderyd Hospital, Karolinska Institutet, Stockholm, 182 88, Sweden.

[*] These authors contributed equally.

Corresponding author: juleen.zierath@ki.se

SUMMARY

Increased levels of branched-chain amino acids (BCAAs) are associated with type 2 diabetes (T2D) pathogenesis. However, most metabolomic studies in T2D are limited to an analysis of plasma metabolites under fasting conditions, rather than the dynamic shift in response to a glucose challenge. Moreover, metabolomic profiles of peripheral tissues involved in glucose homeostasis are scarce and the transcriptomic regulation of genes involved in BCAA catabolism in T2D is partially unknown. Using metabolomic and gene expression approaches, we found that impairments in BCAA catabolism in T2D patients under fasting conditions are exacerbated after a glucose load, concomitant with downregulated expression of BCAA-related genes in skeletal muscle. We identified a key regulatory role for Estrogen-Related Receptor α (ERRα) in PGC-1α-mediated upregulation of BCAA genes and leucine oxidation. Thus, metabolic inflexibility in T2D impacts BCAA homeostasis and the transcriptional regulation of BCAA genes via a PGC-1α/ERRα-dependent mechanism.

KEYWORDS

Branched-chain amino acid, Type 2 diabetes, Skeletal muscle, Estrogen-related receptor alpha, Peroxisome proliferator-activated receptor gamma coactivator 1-alpha, Acylcarnitines, Oral glucose tolerance test.

INTRODUCTION

Type 2 diabetes (T2D) is a chronic metabolic disease characterized by chronic hyperglycemia and insulin resistance (Leahy, 2005). These metabolic derangements severely affect pathways controlling the appropriate sensing and handling of nutrients, thereby leading to a positive energy balance and metabolic inflexibility, which further compromises whole body glucose homeostasis (Galgani et al., 2008). Overnutrition and T2D-related disturbances also affect non-glucose metabolites such as branched-chain amino acids (BCAAs; leucine, isoleucine and valine) (Felig et al., 1969), essential amino acids whose utilization and metabolism are exquisitely regulated in healthy individuals. While BCAA and related metabolites play a role in protein synthesis, they also modulate liver gluconeogenesis and lipogenesis rates, cell growth and nutrient signaling, and can enter the tricarboxylic acid cycle to produce energy (Nie et al., 2018). Under pathological conditions, altered levels of BCAAs, especially in a context of overnutrition, can disrupt insulin sensitivity and secretion (Patti et al., 1998).

Obese, insulin resistant and T2D individuals exhibit higher serum concentrations of BCAAs than their healthy counterparts (Huffman et al., 2009). Metabolomic profiling of blood metabolites has revealed a signature of altered BCAA catabolism in obese individuals, with a strong association with insulin resistance (Newgard et al., 2009). In T2D, BCAA-related metabolites are predictive of disease pathogenesis (Wurtz et al., 2013), as well as prognostic markers for intervention outcomes (Menni et al., 2013; Shah et al., 2012). Moreover, Mendelian randomization analysis suggested a causal link between genetic variants associated to impaired BCAA catabolism and higher risk of T2D (Lotta et al., 2016). Therefore, there is growing evidence that high levels of BCAAs and related intermediate metabolites are not only T2D biomarkers, but also pathophysiological factors. However, the vast majority of these studies were conducted in individuals after an overnight fast, under conditions in which both

protein degradation in skeletal muscle and a concomitant release of amino acids to support gluconeogenesis (Fukagawa et al., 1985) could mask alterations in BCAA homeostasis. Moreover, they do not provide insight into the dynamic shift in metabolism that occurs in response to nutritional challenges. An analysis of metabolomic signatures in fasted glucose tolerant and T2D individuals before and after a glucose challenge may provide insight into dynamic changes in BCAAs and related metabolites and the consequences of insulin resistance.

Skeletal muscle is the largest contributor to systemic BCAA oxidation (Neinast et al., 2019) and therefore impairments in glucose and BCAA metabolism in myocytes has an impact on whole body metabolic homeostasis. While BCAA-related gene expression and oxidation rates are reduced in *vastus lateralis* muscle biopsies from insulin resistant subjects (Lerin et al., 2016), studies of BCAA metabolism in human skeletal muscle are scarce. BCAA catabolism occurs in the mitochondrial matrix, implicating alterations in mitochondrial proteins may influence BCAA metabolism. For example, in transgenic mice overexpressing the mitochondrial biogenesis inducer peroxisome proliferator-activated receptor γ (PPAR γ) coactivator 1α (PGC-1α), BCAA levels are reduced in *gastrocnemius* muscle (Hatazawa et al., 2014). Conversely, administration of the PPARγ agonist thiazolidinedione rosiglitazone improves glycemic control and increases circulating levels BCAAs in individuals with T2D (van Doorn et al., 2007). Nevertheless, mechanisms underlying the role of PGC-1α in the regulation of BCAA catabolism are unclear.

Using metabolomic and transcriptomic approaches, we provide evidence that BCAA catabolism in skeletal muscle is attenuated and further impaired by a metabolic challenge in individuals with T2D. We report that metabolic inflexibility of BCAA catabolism in skeletal muscle is associated with alterations in BCAA gene expression via a PGC-1α/ERRα-dependent mechanism.

RESULTS

Participants

Twenty-seven normal glucose tolerant (NGT) and twenty-eight T2D men were recruited for this study (Figure 1). For the metabolomic analysis, plasma and skeletal muscle biopsies from fifteen NGT individuals (mean ± SEM, age: 59.6 ± 2.4 y; body mass index: 25.95 ± 0.59 kg/m^2; fasting blood glucose: 5.4 ± 0.1 mmol/L) and twenty-six T2D (age: 62.2 ± 1.2 y; body mass index: 27.66 ± 0.47 kg/m^2; fasting blood glucose: 8.6 ± 0.4 mmol/L) were used. For the transcriptional analysis, plasma and skeletal muscle biopsies from twenty-five NGT individuals (age: 57.7 ± 1.8 y; body mass index: 25.98 ± 0.35 kg/m^2; fasting blood glucose: 5.5 ± 0.1 mmol/L) and twenty-five T2D (age: 62.5 ± 1.3 y; body mass index: 27.94 ± 0.48 kg/m^2; fasting blood glucose: 8.6 ± 0.4 mmol/L) were used.

Glucose loading further attenuates BCAA catabolism in T2D patients

Glucose ingestion in fasted subjects elicits an insulin-dependent metabolic response that is blunted in individuals with pre-diabetes (Shaham et al., 2008). To assess whether this impaired response also affects the BCAA profile, we measured levels of leucine, isoleucine, valine, and derived metabolites in plasma and *vastus lateralis* biopsies from NGT and T2D individuals before and after an (OGTT). On average, the three BCAAs were ~10% and ~13% higher in plasma and skeletal muscle from fasted T2D subjects (Figure 2A-C), and non-significant changes were found in the corresponding branched-chain α-keto acids (BCKAs) (Figure 2D-F). While the levels of BCAA-derived acyl-carnitines were not different between groups (Figure 2G-K), 3-hydroxisobutyrate was higher in plasma (+37%) and skeletal muscle (+45%) from T2D subjects (Figure 2L). This valine-derived metabolite has been reported to promote insulin resistance in skeletal muscle cells by increasing fatty acid uptake (Jang et al., 2016).

Glucose ingestion decreased circulating and intramuscular levels of BCAA and BCKA (Figure 2A-F), albeit to a lesser extent in individuals with T2D. The intramuscular content of BCKA was decreased 37–56% in NGT subjects, whereas levels remained unaltered in T2D. While the transamination from BCAA to BCKA is reversible, all three BCKA are irreversibly decarboxylated by the branched-chain α-ketoacid dehydrogenase complex (BCKDH), the rate-limiting enzyme in the catabolism of BCAA. These results suggest that skeletal muscle BCKDH activity is impaired in individuals with T2D. Therefore, we determined total abundance and phosphorylated (inactive) BCKDH content in skeletal muscle (Figure 2M-O). We found that BCKDH abundance and phosphorylation was not altered between NGT and T2D subjects. Given recent evidence that BCAA catabolic flux cannot be predicted by BCKDH phosphorylation status (Neinast et al., 2019), we cannot exclude the possibility that BCKDH activity is impaired based on this Western blot analysis. Conversely, we observed a trend towards an accumulation of BCAA-derived acyl-carnitines in skeletal muscle (Figure 2G-K), including isovalerylcarnitine and isobutyrylcarnitine, with levels increased in T2D as compared to NGT subjects after the OGTT. Moreover, glucose loading induced a significant decrease of 3-hydroxyisobutyrate levels in skeletal muscle of NGT but not T2D subjects. Schematic representation of BCAA degradation pathway and the log2 fold changes of the evaluated metabolites after OGTT relative to fasting conditions in both groups are reported (Figure 2P-Q). Collectively, these results suggest that a glucose challenge unmasks defects at several steps of BCAA catabolism.

Expression of genes involved in BCAA catabolism is decreased in T2D skeletal muscle. We next evaluated whether the metabolic alterations in T2D in response to a glucose challenge are associated with changes in skeletal muscle expression of genes involved in BCAA metabolism. Expression of genes encoding for enzymes involved in first steps of BCAA metabolism, namely Branched Chain Amino Acid Transaminase 2 (*BCAT2*) and three subunits

of the BCKDH complex (Figure 3A) were decreased in skeletal muscle of T2D patients as compared to NGT controls. Furthermore, 69% of the analyzed genes participating in metabolic steps downstream of the oxidative decarboxylation reaction catalyzed by BCKDH showed a similar profile (Figure 3B), indicating that BCAA gene expression is widely downregulated in T2D skeletal muscle. These differences were also evident after an OGTT, as mRNA levels remained relatively stable after glucose loading. Thus, we next determined potential candidates involved in the regulation of BCAA gene expression that could explain the differences between NGT and T2D.

PPARGC1A is downregulated in skeletal muscle from fed and fasted T2D patients.

Skeletal muscle PGC-1α expression is reduced in T2D patients (Patti et al., 2003), and proposed as a potential upstream regulator of BCAA metabolism (Hatazawa et al., 2014). As a transcriptional coactivator, PGC-1α interacts with several transcription factors and nuclear receptors to enhance gene expression. The orphan nuclear receptor ERRα, encoded by *ESRRA*, is a canonical functional partner of PGC-1α (Figure 3C) that regulates metabolic processes in mitochondria including oxidative phosphorylation and metabolism of lipids and ketones (Luo et al., 2003; Svensson et al., 2016). Therefore, we determined the expression of *PPARGC1A* and *ESRRA* in skeletal muscle of NGT and T2D subjects. *PPARGC1A* mRNA was reduced in T2D subjects, whereas *ESRRA* mRNA showed non-significant differences in skeletal muscle of fasted subjects (Figure 3D).

PGC-1α mediates BCAA gene expression in primary human skeletal muscle cells.

We next determined whether PGC-1α mediates BCAA gene expression in skeletal muscle. Primary human skeletal muscle cells (HSMCs) transfected with *PPARGC1A* siRNA had reduced expression of *PPARGC1A* (Figure 4A), which moderately decreased expression of genes of the family of acyl-CoA dehydrogenases (*ACAD8*, *ACADSB*, and *IVD*), and *HIBADH*

(encoding the 3-hydroxyisobutyrate dehydrogenase enzyme) as compared to cells treated with a scramble siRNA (Figure 4B). Conversely, expression of the three BCKDH subunits, *BCKDHB, DBT* and *DLD* remained unaltered. Adenovirus-mediated *PPARGC1A* overexpression (Ad-PGC1A) in HSMCs (Figure 4C) increased the expression of 61% of the analyzed genes relative to adenovirus-GFP control cells, including two of the three BCKDH subunits (Figure 4D). *BCKDK*, which encodes a kinase that phosphorylates and inactivates BCKDH, was upregulated after *PPARGC1A* silencing and unaltered by *PPARGC1A* overexpression, suggesting that not all BCAA genes are equally modulated by PGC-1α.

Paradoxically, BCKDH protein content was significantly lower in Ad-PGC1A overexpressing cells (Figure 4E), leading to an increase in the pBCKDH/BCKDH ratio (Figure 4F-G), despite the higher levels of the phosphatase PPM1K (Figure 4I).

Mice with skeletal muscle-specific modified expression of *PPARGC1A* exhibit altered levels of BCAA gene transcripts and related metabolites.

Next, we used two different mouse models to assess the impact of muscle-specific altered BCAA gene expression in circulating and intramuscular BCAAs. Muscle-specific PGC-1α knockout mice (PGC-1α mKO) had normal body weight (Figure S1A) and slightly impaired glucose tolerance (Figure S1B-C) compared to their wild-type (WT) littermates. Contrasting with the *in vitro* experiments with primary HSMCs (Figure 3), skeletal muscle from PGC-1α mKO mice (Figure 5A) had lower expression of the majority (67%) of the analyzed BCAA genes relative to WT littermates (Figure 5B-D), including genes encoding BCKDH subunits (Figure 5B) and the BCKDH regulatory enzymes PPM1K and BCKDK (Figure 5C). Accordingly, a contrasting profile of BCAA gene expression was observed in skeletal muscle-specific PGC-1α transgenic mice (mTg) versus the PGC-1α mKO mice, with an upregulation of the BCAA gene profile in skeletal muscle as compared to wild-type (WT) littermates (Figure

5E-H). These changes in gene expression were not associated with alterations in either body weight or glucose tolerance (Figure S1D-F). Consistent with our results from human myotubes (Figure 4), the gene encoding for the enzyme responsible for the transamination of BCAA to BCKA was unchanged in all groups, indicating that *BCAT2* transcriptional regulation is PGC-1α-independent.

To ascertain whether PGC-1α-associated alterations in BCAA gene expression have functional implications in BCAA metabolism, we performed LC/MS metabolomics to profile BCAA-related metabolites in plasma and *quadriceps* muscle from mKO and mTG mice and respective WT littermates. Circulating levels of leucine, isoleucine, and valine in mKO and mTG mice were not statistically different when compared to the respective WT littermates (Figure 5I-K), whereas the intramuscular content of valine was reduced in mTG mice (Figure 5L-N). Similar non-significant changes were observed for isoleucine (p=0.09) and isovalerylcarnitine (p=0.12) (Figure 5M and O). Surprisingly, mKO mice exhibited decreased levels of 3-hydroxyisobutyrate (Figure 5Q), although the rest of analyzed metabolites were unaltered compared to WT littermates.

Finally, we determined whether overexpression of *PPARGC1A* would increase BCAA oxidative rates in C2C12 myotubes. Consistent with our results in human myotubes, C2C12 adenovirus-mediated overexpression of *PPARGC1A* upregulated the expression of all analyzed BCAA genes, with the notable exception of *ACADSB* and *BCKDK* (Figure S1G), which also followed a distinct expression pattern in mTG mice. In line with the trend towards lower intramuscular accumulation of BCAA metabolites in the mTG mice, PGC-1α-mediated upregulation of BCAA genes in C2C12 myotubes increased leucine oxidation (Figure S1H).

PGC-1α regulates BCAA gene transcription through ERRα.

As a transcriptional coactivator, PGC-1α does not directly bind DNA in a sequence-specific manner, but interacts with transcription factors and nuclear receptors to enhance gene transcription (Puigserver and Spiegelman, 2003). After confirming the involvement of PGC-1α in the transcriptional regulation of the BCAA metabolism gene set, we next investigated whether the orphan nuclear receptor ERRα was necessary for PGC-1α-enhanced BCAA gene expression. siRNA-mediated silencing of *ESRRA* in primary HSMCs (Figure 6A) decreased the expression of 65% of the analyzed genes (Figure 6B). Notably, *BCAT2* and *BCKDK* were among the unaltered genes. Next, we determined whether this BCAA gene downregulation affects leucine oxidation in skeletal muscle. Differentiated primary HSMCs were treated with either DMSO or 3,6-dichlorobenzo(b)thiophene-2carboxylic acid (BT2). BT2 is a small-molecule inhibitor of BCKDK, and consequently activates the BCKDH complex and increases BCAA oxidative flux. Silencing of *ESRRA* resulted in a significant decrease in leucine oxidation under BCKDH-activated conditions, as measured by CO_2 production after incubation with [U–^{14}C]-leucine (Figure 6C). A schematic biochemical representation of the leucine oxidation assay is shown (Figure 6D).

We next tested the hypothesis that ERRα is a PGC-1α interacting partner in the transcriptional regulation of the BCAA gene set using human differentiated myotubes treated with either scramble siRNA or *ESRRA* siRNA and transfected with adenovirus containing the green fluorescent protein gene (Ad-GFP) or *PPARGC1A* (Ad-PGC-1A). We also tested this hypothesis using *PPARGC1A* overexpressing cells treated with the inverse ERRα agonist XCT-790 (Figure S2). Since *PPARGC1A* and *ESRRA* mutually regulate their expression, we first confirmed that *ESRRA* silencing did not abrogate *PPARGC1A* in cultured cells. Ad-PGC1A cells had high levels of *PPARGC1A* transcripts regardless the treatment with *ESRRA* siRNA (Figure 6H and Figure S1A), whereas the expression of two known targets of PGC-1α/ERRα, *TFAM* and *VEGF*, was dampened by *ESRRA* siRNA despite the overexpression of

PPARGC1A. Similarly, knockdown and inhibition of *ESRRA* completely ablated PGC-1α-mediated upregulation in all analyzed genes (Figure 6E-G, Figure S1B-D), indicating that ERRα is essential for the transcriptomic regulation of the BCAA gene network orchestrated by PGC-1α. A heatmap was constructed showing the fold change in BCAA gene expression in skeletal muscle under the different experimental paradigms used in the current study (Figure 6I).

DISCUSSION

A link between increased plasma BCAAs and insulin resistance was established as early as 1969 (Felig et al., 1969), but this association has remained relatively unexplored until the last decade. We performed a metabolomic and transcriptomic analysis of human plasma and skeletal muscle biopsies, as well as experimental studies in transgenic mouse models and primary HSMCs to elucidate the mechanisms underpinning BCAA metabolism in T2D. While we corroborate the association between BCAA metabolites and T2D (Menni et al., 2013; Suhre et al., 2010; Xu et al., 2013; Yu et al., 2016) and the role of PGC-1α in BCAA catabolism (Hatazawa et al., 2016; Hatazawa et al., 2014; Jang et al., 2016), we provide new evidence that an OGTT unmasks impairments in BCAA catabolism in T2D patients. Moreover, we reveal that PGC-1α-mediated regulation of genes important for BCAA catabolism is dependent on ERRα, a canonical PGC-1α-interacting protein.

Circulating plasma BCAA levels are altered in T2D patients, however metabolomic profiles of peripheral tissues involved in glucose homeostasis are scarce and the transcriptomic regulation of genes involved in BCAA catabolism is unknown. Studies focusing on skeletal muscle BCAA content are limited to an analysis of insulin resistant adults (Lerin et al., 2016), rather than T2D patients. We performed untargeted metabolomic analysis on both plasma and *vastus lateralis* biopsies obtained before and after an OGTT from men with either NGT or T2D. Circulating BCAAs and BCKAs were decreased after an OGTT and this reduction was attenuated in T2D patients, presumably due to insulin resistance, corroborating an earlier study of plasma samples from the Framingham Heart Study Offspring cohort (Ho et al., 2013). In skeletal muscle, insulin inhibits proteolysis (Tessari et al., 1986) and increases the preference for BCAA oxidation (Neinast et al., 2019). Conversely, in the hypothalamus, insulin signaling promotes BCAA catabolism in liver in a glucose-independent manner (Shin et al., 2014), which may explain the reduced BCAA and BCKA metabolism in individuals with T2D as compared

to NGT. Generally, plasma metabolites mirrored skeletal muscle BCAA profile, although greater variation was observed in muscle, possibly due to fiber type heterogeneity of the *vastus lateralis* (Staron et al., 2000). Moreover, the intramuscular accumulation of isovalerylcarnitine, isobutyrylcarnitine, and 3-hydroxyisobutyrate was not reflected in plasma, suggesting defects in processes controlling the export of metabolites from myocytes in T2D. In insulin resistant rodents, BCAA oxidation is shunted from liver and adipose tissue toward skeletal muscle (Neinast et al., 2019). This finding may be clinically relevant, given that the expression of genes regulating BCAA metabolism in skeletal muscle were reduced in T2D patients. In this regard, the accumulation of 3-hydroxyisobutyrate after an OGTT is notable, since this valine-derived metabolite promotes insulin resistance through increased fatty acid uptake in skeletal muscle (Jang et al., 2016). This could lead to a vicious cycle in which secretion of 3-hydroxyisobutyrate from skeletal muscle may decrease insulin sensitivity and further impair insulin signaling. Although elevated levels of circulating C3 and C5 acylcarnitines have been also detected in obese subjects (Newgard et al., 2009), whether accumulation of short-chain acylcarnitines mediates in insulin resistance remains to be elucidated (Schooneman et al., 2013). Nevertheless, these results are suggestive of defects in downstream degradation of BCAA-derived metabolites.

Accumulation of BCAA metabolites in the T2D patients was accompanied by an overall decrease in expression of genes involved in BCAA catabolism, suggesting that alterations in the transcriptional regulation of these genes could lead to attenuated BCAA catabolism in skeletal muscle. Thus, considering that BCAA catabolism occurs within the mitochondrial matrix, we assessed proteins involved in mitochondrial homeostasis. In addition to PGC-1α, which is downregulated in T2D skeletal muscle, we identified the orphan nuclear receptor ERRα as a potential transcription regulator of BCAA-related genes. ERRα is encoded by *ESRRA* and functions as a PGC-1α-interacting partner that coordinates transcriptional

programs controlling energy metabolism (Huss et al., 2004; Mootha et al., 2004). In response to the OGTT, *ESRRA* mRNA was reduced in skeletal muscle from individuals with NGT, but not T2D. Given that ERRα regulates insulin-induced transcriptional responses associated with mitochondrial metabolism (Batista et al., 2019), we next explored whether ERRα and PGC-1α direct the BCAA transcription program.

PGC-1α coordinates metabolic and transcriptomic programs linked to cellular energy homeostasis, such as hepatic gluconeogenesis, lipid metabolism and mitochondrial respiration (Estall et al., 2009; Wu et al., 1999; Yoon et al., 2001). Reduced PGC-1α mRNA and protein are linked to insulin resistance in T2D (Moreno-Santos et al., 2016; Patti et al., 2003). PGC-1α also mediates the expression of genes involved in BCAA catabolism (Hatazawa et al., 2016; Hatazawa et al., 2014; Jang et al., 2016). We found that expression of PGC-1α and several genes involved in BCAA catabolism was reduced in skeletal muscle of T2D patients. Primary HSMCs and mouse skeletal muscle with reduced *PPARGC1A* expression exhibited a mild reduction in several BCAA genes, whereas its overexpression was associated with a consistent upregulation. Thus, while PGC-1α was not essential for basal BCAA gene transcription, it may play a role in the adaptive response to increased BCAA catabolic demands, such as during exercise (Hagg et al., 1982) or nutritional changes. However, some BCAA catabolic genes were unaltered, suggesting that PGC-1α-independent regulatory transcriptional and post-translational mechanisms are also involved. Indeed, overexpression of PGC-1α was associated with reduced BCKDH content, which led to higher phosphorylated BCKDH/total BCKDH ratio despite the increase in PPM1K, a phosphatase responsible for the dephosphorylation of BCKDH. Overall, our results highlight the complexity of the enzymatic networks controlling BCAA metabolism and raise a potential caveat of linking transcriptomic and proteomic data with functional outcomes.

We next hypothesized that alterations in the BCAA gene network would impact BCAA metabolism. We found that mice overexpressing PGC-1α in skeletal muscle exhibited an upregulation of BCAA genes and a trend towards reduced intramuscular accumulation of BCAA metabolites, suggestive of increased BCAA catabolic flux. Accordingly, we found that adenovirus-mediated overexpression of PGC-1α in C2C12 myotubes increased leucine oxidation rates. However, intramuscular levels of BCAA metabolites were unaltered in skeletal muscle of PGC-1α mKO mice. Thus, other organs such as adipose tissue may compensate for a putative impairment in BCAA catabolism (Herman et al., 2010). Furthermore, a metabolic challenge may be necessary to reveal functional alterations in BCAA metabolism in PGC-1α mKO mice.

ERRα physically interacts with PGC-1α to elicit the transcription of genes involved in mitochondrial biogenesis and oxidative phosphorylation (Schreiber et al., 2004), lipid metabolism (Luo et al., 2003) and ketone body homeostasis (Svensson et al., 2016). We found that both *ESRRA* silencing and inverse agonist inhibition of ERRα downregulated BCAA genes and abrogated the *PPARGC1A*-induced responses, indicating ERRα is necessary for the transcription of BCAA genes mediated by PGC-1α. Whether this is due to a direct regulation by binding of the ERRα/PGC-1α complex to potential ERRα response elements (ERREs) in the promoter regions of the analyzed genes warrants further evaluation. A combination of chromatin immunoprecipitation (ChiP) and genomic DNA arrays in mouse cardiac tissue identified 195 promoters bound by ERRα (Dufour et al., 2007), and among these, only ACADM, which also participates in lipid metabolism, is involved in BCAA catabolism. However, ERRα/PGC-1α binds near the transcriptional start site of a previously unidentified gene encoding for the rate-limiting ketolytic enzyme OXCT1 in skeletal muscle (Svensson et al., 2016), suggesting that tissue-specific responses and different bioinformatic approaches could unravel genes directly regulated by ERRα/PGC-1α.

In summary, altered expression of *PPARGC1A*s associated with disturbances in BCAA metabolism in human skeletal muscle of T2D individuals. Experimental approaches to reduce *PPARGC1A* levels partially recapitulates the BCAA gene set profile identified in skeletal muscle from T2D patients (Figure 6H). Our results have clinical relevance and suggest that people with T2D have metabolic inflexibility in regard to BCAA homeostasis and an associated impaired transcriptomic response. Additionally, our data demonstrate that ERRα is essential for PGC-1α-mediated transcriptional regulation of genes involved in BCAA metabolism, either directly or indirectly, thereby unraveling a novel role for this orphan nuclear receptor.

LIMITATIONS OF STUDY

The T2D patients in our study were slightly older and had significantly higher BMI and waist circumference than the controls, which are confounding variables and may affect other pathophysiological processes. Nevertheless, these clinical features are characteristic of the general T2D population (Public Health England, 2012). Moreover, our analysis was limited to male participants, and therefore we cannot exclude sex-specific differences in the analyzed outcomes. Due to limitations in the LC/MS methodology, quantitation of BCAA metabolites with CoA moieties was not possible. To overcome this, we used specific derived carnitines from these metabolites as a proxy, limiting the understanding of how the different conditions affect BCAA catabolism after BCKA decarboxylation. Moreover, alterations in PGC-1α expression may influence fiber type distribution in mouse models (Handschin et al., 2007; Lin et al., 2002), which could impact the results. Nevertheless, similar results were obtained in transgenic mice, *in vitro* primary HSMCs and C2C12 myotubes strongly suggesting that alterations in BCAA metabolism was not due to changes in fiber type.

ACKNOWLEDGMENTS

The costs of human metabolomics study was supported by grant from Daiichi Sankyo Co., Ltd. This work was supported by grants from the Novo Nordisk Foundation (NNF14OC0011493, NNF14OC0009941, NNF18CC0034900), Swedish Diabetes Foundation (DIA2018-357), Swedish Research Council (2015-00165, 2018-02389), the Strategic Research Programme in Diabetes at Karolinska Institutet (2009-1068), the Knut and Alice Wallenberg Foundation (2018-0094) and the Stockholm County Council (SLL20170159). David Rizo-Roca is supported by a Novo Nordisk postdoctoral fellowship run in partnership with Karolinska Institutet.

AUTHOR CONTRIBUTIONS

R.J.O.S. conceived the idea, planned the experiments and collected and analyzed data. D.R.R performed leucine oxidation assays, analyzed data and wrote the manuscript. A.V.C. contributed to discussion and reviewed the manuscript. E.C. collected mouse metabolite data and contributed to discussion. R.F. assisted with animal care, oral glucose tolerance tests and skeletal muscle sampling. S.K. contributed to the conception of the idea. J.H. contributed to the conception of the idea. H.K.K. assisted with recruitment and collection of human metabolite data. C.H. provided mouse biological samples. T.M. supervised acquisition and analysis of mouse metabolite data. A.K. supervised the study and reviewed the manuscript. E.N. assisted with recruitment and obtained human skeletal muscle biopsies and blood samples. J.R.Z. supervised the study, reviewed and edited the manuscript and acquired funding.

DECLARATION OF INTERESTS

J.H. is employee of Daiichi Sankyo Co., Ltd.

FIGURE TITLES AND LEGENDS

Figure 1. Flow chart illustrates subject enrolment and analysis. Sixty-one individuals were assessed for eligibility, six of which were excluded for not meeting the inclusion criteria. Group size for transcriptomic and metabolomic analysis is reported. Transcriptomic and metabolomic analysis shared 13 NGT subjects and 23 T2D.

Figure 2. Glucose loading further attenuates BCAA catabolism in T2D patients. Boxplots show scaled intensity values of BCAAs **(A-C)**, BCKAs **(D-F)**, BCAA-derived carnitines **(G-K)** and valine-derived 3-hydroxisobutyrate **(L)** in plasma and skeletal muscle from NGT and T2D subjects, before and after an OGTT. **M)** Western blot of BCKDH and its inactivated, phosphorylated form pBCKDH **(N)** before and after OGTT in skeletal muscle biopsies from NGT and T2D individuals (n = 10 each). Inter-membrane comparison was carried out by loading a control sample in all membranes. **O)** Representatives immunoblot bands of the analyzed proteins. **P)** Catabolic pathways of BCAAs and genes codifying for involved enzymes (in white boxes). Metabolites in bold are shown in figures A-L. Dashed arrows indicate intermediate metabolites are not shown. **Q)** Heatmap representing positive (red) and negative (blue) fold change variations after OGTT relative to fasting levels. Statistical analysis was performed using two-way mixed-design ANOVA followed by Sidak's post-hoc test (NGT, n=15; T2D, n=26). *, statistically significant difference between fasting and OGTT; † statistically significant difference between T2D and its NGT counterpart. GL×C indicate statistical interaction between the OGTT glucose load (GL) and condition (C). One, two and three symbols indicate p-value <0.05, <0.01 and <0.001, respectively. BCAA, branched-chain amino acid; BCKA, branched-chain α-keto acid; NGT, normal glucose tolerant; T2D, type 2 diabetic; OGTT, oral glucose tolerance test.

Figure 3. Expression of genes involved in BCAA catabolism is decreased in T2D skeletal muscle. Expression of genes encoding the mitochondrial transaminase BCAT2 and three subunits of the BCKDH complex **(A)** and several BCAA catabolic enzymes **(B)** in skeletal muscle biopsies from NGT and T2D subjects before and after an OGTT. **C)** STRING Interacting Network showing top 5 interacting proteins for PGC-1α. Line thickness indicates the strength of data support. **D)** Expression of the transcriptional coactivator *PPARGC1A* and its interacting partner *ESRRA* in muscle biopsies from NGT and T2D subjects. Gene expression is shown as log2(fold-change) normalized to the NGT Fasting group. Statistical analysis was performed using two-way mixed-design ANOVA followed by Sidak's post-hoc test (n=25) on dCt values. *, statistically significant difference between T2D and its fasting or OGTT NGT counterpart; †, statistically significant difference between fasting and OGTT. GL×C indicate statistical interaction between the OGTT glucose load (GL) and condition (C). One, two and three symbols indicate p-values <0.05, 0.01 and 0.001, respectively. NGT, normal glucose tolerant; T2D, type 2 diabetic; OGTT, oral glucose tolerance test; F, fasting, O, OGTT.

Figure 4. PGC-1α mediates BCAA gene expression in human skeletal muscle cells. **A)** Efficiency of *PPARGC1A* siRNA-mediated silencing in HSMCs. **B)** Effects of the silencing of *PPARGC1A* on the expression of BCAA catabolic genes, BCKDK and PPM1K in HSMCs. **C)** Adenovirus-mediated overexpression of *PPARGC1A* (Ad-PGC1A) in HSMCs. **D)** Effects of Ad-PGC1A on the expression of BCAA catabolic genes, BCKDK and PPM1K in HSMCs. **E-I)** Western blot of BCKDH **(E)**, its inactivated, phosphorylated form pBCKDH **(F)** and ratio **(G)**, and their kinase BCKDK **(H)** and phosphatase PPM1K **(I)** expressed as arbitrary units in adenovirus-mediated *PPARGC1A* overexpressing HSMCs. **J)** Representatives immunoblot bands of the analyzed proteins. Arrow indicates the band corresponding to PPM1K protein. Gene expression is shown as log2(fold-change) normalized to controls (dotted line). Statistical analysis was performed using paired t-test on dCt values (n=6) and band intensity (n=6). *, **

and *** represent p<0.05, <0.01 and 0.001 vs. scr (A-B) and Ad-GFP (C-I); respectively. siRNA, small interfering RNA; scr, scrambled siRNA; Ad-GFP, adenoviral overexpression of green fluorescent protein. ◦, values greater than 1.5 times the interquartile range plus the 75th percentile; •, significant outliers not considered in statistical calculations.

Figure 5. Mice with skeletal muscle-specific modified expression of *PPARGC1A* exhibit altered levels of BCAA gene transcripts and related metabolites. A) Gene expression of *PPARGC1A* in muscle-specific *PPARGC1A* knockout mice (mKO). **B-D)** Expression of genes encoding the mitochondrial transaminase BCAT2 and three subunits of the BCKDH complex **(B)**, BCKDH regulatory enzymes BCKDK and PPM1K **(C)** and BCAA catabolic enzymes **(D)** in mKO mice. **E)** Gene expression of *PPARGC1A* in muscle-specific *PPARGC1A* transgenic mice (mTG). **F-H)** Expression of genes encoding the mitochondrial transaminase BCAT2 and three subunits of the BCKDH complex **(F)**, BCKDH regulatory enzymes BCKDK and PPM1K **(G)** and BCAA catabolic enzymes **(H)** in mTG mice. **I-K)** Circulating levels of leucine, isoleucine and valine in plasma from mKO, mTG and correspondent WT littermates. **L-Q)** Intramuscular levels BCAA and downstream intermediate metabolites in quadriceps muscle from mKO, mTG and correspondent WT littermates. Gene expression is shown as log2(fold-change) normalized to WT animals. The dotted line represents the mean of the WT group. Statistical analysis was performed using unpaired t-test on dCt values (A-H) or scaled intensity (I-Q). *, ** and *** represent p<0.05, <0.01 and 0.001 vs. WT counterpart, respectively. Group size in gene expression experiments and metabolite analysis was as follows: mKO and corresponding WT littermates, n=9; mTG and corresponding WT littermates, n=6 (with the exception of isovalerylcarnitine (O) and tyglylcarnitine (P), in which 4 samples per group were analyzed). WT, wild type; mKO, muscle-specific PGC-1α knockout mice; mTG, muscle-specific PGC-1α transgenic mice; OGTT, oral glucose tolerance test. ◦,

values greater than 1.5 times the interquartile range plus the 75th percentile; •, significant outliers not considered in statistical calculations. See also Figure S1.

Figure 6. PGC-1α regulates BCAA gene transcription through ERRα. A) Efficiency of *ESRRA* siRNA-mediated silencing. **B)** Silencing of *ESRRA* on decreases the expression of BCAA catabolic genes, BCKDK and PPM1K in HSMCs. **C)** Silencing of *ESRRA* reduces BT2-stimulated leucine oxidation in HSMCs. **D)** Schematic biochemical representation of the leucine oxidation assay, in which release $^{14}CO_2$ is trapped and counted. **E-G)** BCAA gene expression in adenovirus-mediated *PPARGC1A* (Ad-PGC1A) overexpressing cells with or without *ESRRA* silencing. **H)** Effects of adenovirus-mediated *PPARGC1A* overexpression in cells transfected with *ESRRA* siRNA on the expression of *ESRRA*, *PPARGC1A* and its well-established downstream target genes *TFAM* and *VEGF*. **I)** Heatmap showing a summary of fold change BCAA genes expression in the different experimental models used in the current study. Overall, models in which *PPARGC1A* expression was reduced mimicked BCAA gene set profile from T2D skeletal muscle. Gene expression is shown as log2(fold-change) normalized to the control samples (dotted line) scr (A-B) or scr-Ad-GFP (C-F). Statistical analysis was performed using paired t-test (A-B, n=7) or two-way repeated measures ANOVA followed by Tukey's post-hoc test (E-H, n=6) on dCt values. *, ** and *** represent $p<0.05$, <0.01 and 0.001 vs. scr (A-B) or scr-Ad-GFP (C-F); respectively. p(OE×siESRRA) indicates statistical significance of the interaction between *PPARGC1A* overexpression and *ESRRA* silencing. Specific significant differences between groups are not shown in cases where statistically significant interaction was found. siRNA, small interfering RNA; Ad-GFP, adenoviral overexpression of green fluorescent protein; BT2, 3,6-dichlorobrenzo(b)thiophene-2carboxylic acid; scr, scrambled siRNA; TCA, tricarboxylic acid cycle. See also Figure S2.

TABLES WITH TITLES AND LEGENDS

Table 1. Clinical characteristics of the subjects included in the metabolomic analysis.

	NGT	T2D	P-value
Age	59 ± 2.4	62 ± 1.2	0.1611
Weight [kg]	81 ± 2.7	88 ± 1.8	0.0209
Height [m]	1.77 ± 0.02	1.79 ± 0.01	0.4082
BMI [kg/m^2]	25.95 ± 0.59	27.66 ± 0.47	0.0307
Waist [cm]	90 ± 1.6	100 ± 1.6	0.0002
Hip [cm]	97 ± 1.2	101 ± 1.2	0.0241
W/H ratio	0.93 ± 0.01	0.99 ± 0.01	0.0008
Pulse [BPM]	62 ± 2.0	68 ± 1.6	0.0234
FP-glucose [mmol/L]	5.41 ± 0.13	8.59 ± 0.37	<0.0001
120 min-glucose [mmol/L]	6.05 ± 0.25	16.66 ± 0.58	<0.0001
HbA1c [mmol/mol]	36.13 ± 1.13	51.19 ± 1.32	<0.0001
S-insulin [pmol/L]	52.37 ± 5.30	85.51 ± 9.06	0.0124
120 min S-Insulin [pmol/L]	294.2 ± 43.41	327.5 ± 42.06	0.6155
P-Creatinine [µmol/L]	84.53 ± 2.65	80.72 ± 2.17	0.2794
P-ASAT [µkat/L]	0.42 ± 0.04	0.39 ± 0.03	0.5992
P-ALAT [µkat/L]	0.38 ± 0.06	0.48 ± 0.04	0.1161
P-TG [mmol/L]	1.08 ± 0.14	1.41 ± 0.13	0.1093
P-Chol [mmol/L]	5.27 ± 0.17	4.50 ± 0.14	0.0014
P-HDL [mmol/L]	1.33 ± 0.06	1.24 ± 0.06	0.3562
P-LDL [mmol/L]	3.47 ± 0.13	2.62 ± 0.14	0.0003
S-C-peptide [nmol/L]	0.69 ± 0.04	0.99 ± 0.08	0.0115
HOMA1-IR	1.71 ± 0.22	5.28 ± 0.65	0.0013

Results are mean ± SEM for Normal Glucose Tolerant (NGT; n=15) and Type 2 Diabetic (T2D; n=26) men. Statistical analysis was performed using Student's *t*-test.

Table 2. Clinical characteristics of the subjects included in the transcriptomic analysis.

	NGT	T2D	P-value
Age	58 ± 1.8	62 ± 1.3	0.0185
Weight [kg]	84 ± 1.7	89 ± 1.9	0.0314
Height [m]	1.80 ± 0.02	1.79 ± 0.01	0.7185
BMI [kg/m^2]	25.98 ± 0.35	27.94 ± 0.48	0.0020
Waist [cm]	93 ± 1.4	101 ± 1.7	0.0020
Hip [cm]	99 ± 0.9	101 ± 1.3	0.1691
W/H ratio	0.94 ± 0.01	0.99 ± 0.01	0.0009
Pulse [BPM]	61 ± 1.4	68 ± 1.6	0.0072
FP-glucose [mmol/L]	5.46 ± 0.08	8.56 ± 0.39	<0.0001
120 min-glucose [mmol/L]	5.89 ± 0.27	16.20 ± 0.69	<0.0001
HbA1c [mmol/mol]	35.76 ± 0.64	50.44 ± 1.50	<0.0001
S-insulin [pmol/L]	52.71 ± 5.58	92.58 ± 9.01	0.0008
120 min S-Insulin [pmol/L]	314.9 ± 50.8	350.5 ± 42.4	0.5937
P-Creatinine [µmol/L]	83.64 ± 2.36	79.71 ± 2.29	0.2307
P-ASAT [µkat/L]	0.38 ± 0.03	0.40 ± 0.03	0.7613
P-ALAT [µkat/L]	0.42 ± 0.05	0.50 ± 0.04	0.2565
P-TG [mmol/L]	1.25 ± 0.15	1.43 ± 0.13	0.4415
P-Chol [mmol/L]	5.40 ± 0.20	4.48 ± 0.15	0.0005
P-HDL [mmol/L]	1.30 ± 0.05	1.19 ± 0.06	0.1709
P-LDL [mmol/L]	3.56 ± 0.17	2.63 ± 0.15	0.0002
S-C-peptide [nmol/L]	0.69 ± 0.04	1.03 ± 0.08	0.0008
HOMA1-IR	1.86 ± 0.21	5.23 ± 0.65	<0.0001

Results are shown as mean ± SEM. Normal Glucose Tolerant (NGT; n=25) and Type 2 Diabetic (T2D; n=25) men. Statistical analysis was performed using Student's *t*-test.

STAR METHODS

Lead Contact and Resource Sharing

Further information and requests for resources or reagents should be directed to and will be made available upon reasonable request by the Lead Contact, Juleen R. Zierath, (Juleen.Zierath@ki.se).

Materials Availability

This study did not generate new unique reagents.

Data and Code Availability

****

Experimental Model and Subject Details

Subject characteristics

Thirty-two men with NGT and twenty-nine men with T2D aged 44-69 years were recruited to participate in this study. The study was approved by the regional ethical review board in Stockholm. All participants gave oral and written consent to participate in the study. The experimental procedures were conducted according to the Declaration of Helsinki. Participants underwent a clinical health screening consisting of clinical chemistry and anthropometric measurements (Table 1 and 2). After clinical health screening, five individuals initially characterized as NGT and one individual previously diagnosed as T2D were diagnosed as impaired glucose tolerant and excluded from the study (Figure 1).

Subjects with T2D had higher blood glucose and Hb1Ac and HOMA-IR, as well as higher BMI and waist circumference (Table 1 and 2). Moreover, the men with T2D included in the transcriptomic analysis were older than the men with NGT (Table 2).

Primary human skeletal muscle cells culture

Human satellite cells were harvested from *vastus lateralis* skeletal muscle biopsies of healthy male and female volunteers as described (Al-Khalili et al., 2003). Cells were propagated in growth media (F12/DMEM, 20% FBS, and 1% anti-anti) until ~90% confluence was reached. Cells were then differentiated for 4 days with fusion media (DMEM/M199 (4:1), 1% FBS, 1% anti-anti, 20 mM HEPES, 0.03 µg/mL $ZnSO_4$, 1.4 µg/mL vitamin B12, 10 µg/mL insulin, and 100 µg/mL apo-transferrin). Thereafter, myotubes were cultured in post-fusion media (DMEM/M199 (4:1), 1% FBS, 1% anti-anti, 20 mM HEPES, 0.03 µg/mL ZnSO4, and 1.4 µg/mL vitamin B12). Cultures were incubated at 37°C in 7.5% CO_2 humidified chambers, and medium was changed every second day during growth and differentiation.

C2C12 cell culture

Mouse C2C12 myoblasts (ATCC, VA) were propagated in growth media (DMEM, 20% FBS, and 1% anti-anti) and seeded at density of 42 000 cells/cm^2. After ~12 hours, the culture medium was changed to differentiation medium (DMEM, 2% horse serum, and 1% anti-anti). Cells were incubated at 37°C in 5% CO_2 humidified chambers, and medium was changed every second day during growth and differentiation. C2C12 cells were differentiated for six days before final experiments.

Mouse models

Mice were housed under controlled lighting (12 h light/12 h dark cycle) with free access to food and water. Experiments were performed in accordance with Swiss federal guidelines and were approved by the Kantonales Veterinäramt Basel-Stadt. Skeletal muscle-specific PGC-1α transgenic (mTG) mice are described elsewhere (Lin et al., 2002). The PGC-1α muscle-specific knockout (mKO) mice were generated by breeding PGC-1$\alpha^{loxP/loxP}$ mice (Lin et al., 2004) with transgenic mice expressing the Cre recombinase under the control of the human α-skeletal actin

promoter (HSA-Cre) . Male mice aged between 11–14 weeks were used in all experiments. Chow diet (AIN-93G; 7% fat, 58.5% carbohydrates, and 18% protein) was provided by Provimi Kliba AG (Kaiseraugst, Switzerland).

Method Details

Blood and muscle biopsy sampling and oral glucose tolerance test

Participants arrived at the clinic at 07:45 after a 12-h fasting period. A catheter was inserted into an arm vein and fasting blood samples were obtained. After applying local anesthesia (Lidokain hydrochloride 5 mg/mL), a 1 cm incision was made in the skin and fascia of the *vastus lateralis* portion of the quadriceps muscle using a conchotome (AgnTho's AB, Sweden). Muscle biopsies were immediately rinsed in ice-cold PBS solution, blotted on a filter paper to dry off excessive liquid and immediately snap-frozen in liquid nitrogen. After ∼15 min, participants were given a standardized solution containing 75 g of glucose. A second blood sample was obtained 30 min after glucose ingestion. Finally, 120 minutes after glucose ingestion another blood sample and a second skeletal muscle biopsy were obtained. All biopsies were kept in liquid nitrogen storage until analysis.

Human plasma and skeletal muscle metabolomics

Metabolomic analysis was performed by Metabolon, Inc. (Durham, NC) as previously described (Evans et al., 2009). Briefly, the protein fraction was removed using a methanol extraction method while allowing maximum recovery of small molecules. The resulting extract was divided into five fractions: one for analysis by ultra-high-performance liquid chromatography-tandem mass spectroscopy (UPLC-MS/MS) with positive ion mode electrospray ionization, one for UPLC-MS/MS with negative ion mode electrospray ionization, one for liquid chromatography (LC) polar platform, one for analysis by gas chromatography–MS (GC–MS), and one sample was reserved as a backup.

The LC/MS portion of the UPLC-MS/MS platform was based on a Waters ACQUITY UPLC and a Thermo Scientific Q-Exactive high resolution/accurate mass spectrometer interfaced with a heated electrospray ionization source and Orbitrap mass analyzer operated at 35,000 mass resolution. Separated dedicated columns (Waters UPLC BEH C18-2.1x100 mm, 1.7 µm) were used to perform analysis under acidic positive ion optimized conditions and basic negative ion optimized conditions. The third aliquot was analyzed via negative ionization following elution from a HILIC column (Waters UPLC BEH Amide 2.1x150 mm, 1.7 µm) using a gradient consisting of water and acetonitrile with 10 mM ammonium formate.

Samples destined for GC-MS analysis were dried under vacuum for at least 18 h prior to being derivatized under dried nitrogen using bistrimethyl-silyltrifluoroacetamide. Derivatized samples were separated on a 5% diphenyl / 95% dimethyl polysiloxane fused silica column (20 m x 0.18 mm ID; 0.18 µm film thickness) with helium as carrier gas and a temperature ramp from 60° to 340°C within a 17.5-min period. Samples were analyzed on a Thermo-Finnigan Trace DSQ fast-scanning single-quadrupole mass spectrometer using electron impact ionization and operated at unit mass resolving power. The scan range was from 50–750 m/z.

Compounds were identified by comparison to library entries of purified standards or recurrent unknown entities. Metabolon maintains a library based on authenticated standards that contains the retention time/index (RI), mass to charge ratio (m/z), and chromatographic data on all molecules present in the library. Biochemical identifications were based on three criteria: retention index within a narrow RI window of the proposed identification, accurate mass match to the library and the MS/MS forward and reverse scores between the experimental data and authentic standards. The MS/MS scores were based on a comparison of the ions present in the experimental spectrum to the ions present in the library spectrum.

Mouse plasma and skeletal muscle metabolomics

Mouse sample preparation and analysis was performed at the Swedish Metabolomics Centre (Umeå University). Prior to gas chromatography time-of-flight mass spectrometry (GC-TOF/MS) analysis, a two-step derivatization procedure was carried out to increase metabolites volatility and reduce number of tautomeric forms. The derivatized samples were analyzed on an Agilent 6890 gas chromatograph equipped with a 10 m × 0.18 mm i.d. fused silica capillary column with a chemically bonded 0.18-µm DB 5-MS stationary phase (J&W Scientific, Folsom, CA). The injector temperature was 270°C. The column temperature was held at 70°C for 2 min, increased by 40°C min^{-1} to 320°C, and held there for 1 min. The column effluent was introduced into the ion source of a Pegasus III time-of-flight mass spectrometer, GC-TOF/MS (Leco, St. Joseph, MI, USA). The transfer line and the ion source temperatures were 250 and 200°C, respectively. Ions were generated by a 70-eV electron beam at an ionization current of 2.0mA. The spectra were recorded in the mass range 50–800 m/z at a rate of 30 spectra s^{-1}.

Samples destined to liquid chromatography time-of-flight mass spectrometry (LC-TOF/MS) were re-suspended in methanol and water (1:1) and injected onto a Waters Acquity UPLC HSS T3 C18 column (2.1 × 50 mm, 1.8 µm, Waters, Milford, MA) in combination with a 2.1 mm x 5 mm, 1.8 µm VanGuard precolumn (Waters Corporation, Milford, MA) held at 40°C. Metabolites chromatographic separation were carried out using a gradient solvent system consisting of water with 0.1 % formic acid and acetonitrile/isopropanol (75/25, v/v) with 0.1 % formic acid at a flow rate of 0.5 mL min^{-1}. The detection of separated metabolites was performed using the Agilent 6550 Q-TOF mass spectrometer equipped with a jet stream electrospray ionization source, operating in both positive and negative ion modes. A reference interface was connected for accurate mass measurements; the reference ions purine (4 µM) and HP-0921 (Hexakis (1H, 1H, 3H-tetrafluoropropoxy) phosphazine) (1 µM) were infused directly into the MS at a flow rate of 0.05 mL min-1 for internal calibration. Full scan MS

spectra were collected in a centroid mode over the mass range 70-1700 m/z with an acquisition rate of 4 spectra s^{-1}. The Auto MS/MS was performed on QC-samples. The isolation width was set to narrow, i.e. approx. 1.3 amu, the mass range was 40-1700, and data was collected in centroid mode with an acquisition rate of 3 scans s-1. The collision energy was 10, 20 and 40 ev. Data were acquired with MassHunter Acquisition Software B.07.01.

The processing of GC-TOF/MS data and extraction of putative metabolites was conducted as described (Chorell et al., 2016). Briefly, an in-house MATLAB script was used for the extraction of putative metabolites by matching the mass spectra and retention indices to in-house mass spectral library at the Swedish Metabolomics Centre and the publicly available Max Planck Institute library in Golm. The processing of LC-TOF/MS data and extraction of putative metabolites and lipids were performed by MassHunter Profinder version B.08.00 in combination with Qualitative Analysis software version B.07.00, PCDL manager version B.07.00 and Mass Profiler Professional™ 13.0 (all from Agilent Technologies Inc., Santa Clara, CA). Annotation of metabolites were done by matching the retention time (MS and MS-MS spectra) against the in-house metabolite library.

Small interference RNA silencing of *PPARGC1A* and *ESRRA*

Small interfering RNAs (siRNA) targeting *PPARGC1A* or *ESRRA* mRNA predesigned by ThermoFisher Scientific (Silencer® Select, s21395 and s4830, respectively) were used to knock down the expression of these genes. Scramble siRNA (4390847, ThermoFisher) was used as negative control. Transfection of C2C12 myoblasts and human skeletal muscle cells was performed 3 and 6 days after induction of differentiation, respectively.

Transfections were performed for 5 hours in OptiMEM reduced serum media with Lipofectamine® RNAiMAX according manufacturer's protocol. A second transfection was

conducted after 48 hours and all experimental assays were performed 2 days after the second transfection.

Adenovirus-mediated PGC-1α overexpression

Adenoviral-delivery of either human PGC1a (Ad-PGC1a) or GFP (Ad-GFP) was performed over-night (~16 hours) in differentiated human primary skeletal muscle cells. C2C12 myotubes were transduced over-night (~16 hours) with mouse PGC1a (Ad-PGC1a) or GFP (Ad-GFP) at 50 PFU/cell. The amount of virus (PFU/cell) was not determined for human skeletal muscle cells, since they were still proliferating when seeded to 6-well plates. Instead a PFU of approximately 15×10^6 was used per 6-well plate for human skeletal muscle cells. Experiments on transduced human and mouse cells were performed 48 hours after inducing transduction. In cells that were both treated with siRNA and transduced, silencing was performed as described above and cells were transduced immediately after the second transfection.

RNA isolation and relative mRNA expression

Total RNA from human skeletal muscle biopsies, mouse skeletal muscles and cultured myotubes was extracted using TRIzol according to manufacturer's instructions (Thermo Fisher Scientific). Concentration and extraction quality of RNA samples were determined by spectrophotometry using a Nanodrop ND-1000 (Thermo Fisher Scientific) and equal amounts of RNA were used for cDNA synthesis. cDNA was synthesized using the High Capacity cDNA Reverse Transcription kit with random primers (Thermo Fisher Scientific). RT-qPCR was performed using either a ViiA 7 Real-Time PCR 384-well system or a StepOne Plus Real-Time PCR 96-well system (Thermo Fisher Scientific). Gene expression was determined using Fast SYBR™ Green Master Mix (Thermo Fisher Scientific). Sequences of primers used for the real-time PCR are reported in Tables S1 and S2. Gene expression in human skeletal muscle biopsies and cultured myotubes was normalized to the geometrical mean of *GUSB*, *RPLP0* and *TBP*

expression. For C2C12 cells and mouse tibialis anterior muscle, gene expression was normalized to the geometrical mean of *B2M*, *RPLP0* and *TBP* expression. Relative gene expression was calculated by the comparative ΔΔCt method and normalized to control group (in human and mouse samples, NGT Fasting and WT mice, respectively) or control samples (*in vitro* experiments, cells from each donor were normalized against their correspondent siRNA scr-treated counterparts).

Western blot analysis

Human skeletal muscle biopsies were homogenized in ice-cold lysis buffer [137 mM NaCl, 2.7 mM KCl, 1 mM MgCl2, 0.5 mM Na_3VO_4, 10% (vol/vol) glycerol, 1% (vol/vol) Triton X-100, 20 mM Tris, 10 mM NaF, 1 mM EDTA, 1 mM PMSF, and 1% (vol/vol) protease inhibitor cocktail set 1 (Merck, Darmstadt, Germany)] using a TissueLyser II (21 Hz, 45 sec, two times. Qiagen, Haan, Germany). Homogenates were rotated for 30 min at 4°C and thereafter subjected to centrifugation at 12000 g for 15 min at 4°C.

Cells were lysed in ice-cold homogenization buffer. Lysates were rotated for 30 min at 4°C and subjected to centrifugation at 12000 g for 15 min at 4°C.

Protein concentration in the supernatants of skeletal muscle homogenates and cell lysates was determined by BCA protein assay kit (Pierce Biotechnology, Rockford, IL). Samples were prepared with Laemmli buffer to equal final protein concentrations, separated on Criterion XT Bis-Tris Gels for SDS-PAGE (Bio-Rad, Hercules, CA) and transferred to PVDF membranes (Merck). Thereafter, membranes were stained with Ponceau S to verify transfer quality and confirm equal protein loading. After blocking with 7.5% nonfat milk in Tris-buffered saline with Tween (TBST; 10 mM Tris·HCl, 100 mM NaCl, 0.02% Tween 20) for 2 h at room temperature, membranes were incubated overnight at 4°C with primary antibodies against β-actin, GAPDH, BCKDHA, p^{S293}-BCKDHA, BCKDK, and PPM1K (see Key Resources Table

for more details). Membranes were washed with TBST and incubated with horseradish peroxidase-conjugated secondary antibodies and proteins were visualized by enhanced chemiluminescence (Amersham ECL Western Blotting Detection Reagent, Little Chalfont, UK). Bands of interest were semi-quantified by densitometry (QuantityOne, Bio-Rad).

Leucine oxidation assays

Differentiated muscle cells were washed with PBS and incubated in 6-well plates with 1 ml of Ham's F10 Medium in the presence of 0.1 mCi/ml radiolabeled leucine (L-[U-C14]-Leucine; PerkinElmer) and either 3,6-dichlorobenzo(b)thiophene-2carboxylic acid (BT2) (Sigma-Aldrich) or dimethyl sulfoxide (DMSO). Small cups were carefully placed in the center of cell-culture wells and plates were air-tight sealed. After a 4-hour incubation at 37°C, 150 µL 2 M HCl and 300 µL of 2 M NaOH were added into each well and the small cup, respectively. After 1 hour, the CO_2 released from this reaction was collected into the small cup and subjected to scintillation counting. Data were normalized to the protein content (BCA assay, Bio-Rad).

XCT-790 treatment

Primary HSMCs were transduced overnight with either Ad-GFP or Ad-PGC-1α. Thereafter, cells were incubated with 5 µM of XCT-790, an inverse ERRα agonist, for 32 hours.

Quantification and Statistical Analysis

Data in tables are shown as means ± SEM. Metabolites and gene expression results are shown as Tukey boxplots with median (line), 25–75% (box) and the 25th/75th percentile minus/plus 1.5 times the inter-quartile distance, respectively (whiskers). Values outside this range are plotted as individual white dots. Outlier values detected using the Grubb's test are plotted as black dots and were not considered in the statistical analysis. Gene expression, metabolite and protein results derived from human plasma and skeletal muscle biopsies before and after OGTT were analyzed using two-way mixed-design ANOVA followed by Sidak's *post-hoc* test. Gene

expression and metabolite results derived from the mouse samples were analyzed using an unpaired Student's *t*-test. Gene expression and protein results derived from *in vitro* experiments were analyzed using paired Student's *t*-test or two-way repeated measures ANOVA followed by Tukey's *post-hoc* test. Statistical parameters and additional details can be found in the correspondent figure legends. Graph Pad Prism 8 software was used for statistical analysis.

SUPPLEMENTAL INFORMATION TITLES AND LEGENDS

Figure S1 (Supplementary to Figure 5). A) Body weight of mKO animals and WT littermates (n=9). **B-C)** Oral glucose tolerance test and corresponding area under the curve of mKO animals and WT littermates (n=4). **D)** Body weight of mTG animals and WT littermates (n=6). **E-F)** Oral glucose tolerance test and corresponding area under the curve of mTG animals and WT littermates (n=4). **G)** BCAA gene expression in C2C12 with adenovirus-mediated overexpression of *PPARGC1A* (n=4). **H)** Leucine oxidation in C2C12 with adenovirus-mediated overexpression of *PPARGC1A* (n=4).

Figure S2 (Supplementary to Figure 6). A) Effects of adenovirus-mediated *PPARGC1A* overexpression in cells treated with the *ERRα* inverse agonist XCT-790 on the expression of *ESRRA*, *PPARGC1A* and its well-established downstream target genes *TFAM* and *VEGF*. **B-D)** BCAA gene expression in adenovirus-mediated *PPARGC1A* overexpressing cells treated with vehicle or XCT-790. Gene expression is shown as log2(fold-change) normalized to the scr-Ad-GFP (dotted line). Statistical analysis was performed using paired t-test (A-C, n=7) or two-way repeated measures ANOVA followed by Tukey's post-hoc test (C-F, n=6) on dCt values. *, ** and *** represent $p<0.05$, <0.01 and 0.001 vs. scr-Ad-GFP; respectively. p(OE & XCT-790) indicates statistical significance of the interaction between *PPARGC1A* overexpression and XCT-790 silencing. siRNA, small interfering RNA; scr, scrambled siRNA; Ad-GFP, adenoviral overexpression of green fluorescent protein.

Table S1. Forward and reverse sequences of primers used in gene expression experiment analysis of human skeletal muscle.

Gene	Forward sequence (5' to 3')	Reverse sequence (5' to 3')
ACAD8	CAGGAGGAGAGGAAGGATGC	AGTGTGGGTTCTACTCCTGA
ACADM	ACCAGACCTGTAGTAGCTGC	GAATCAACCTCCCAAGCTGC
ACADSB	AGGCTGCTAAGAAGAAATTTCCT	GTAAATGTTTGCAGGGGAGC
ALDH1B1	AACCAGAACCCAAGCGTGAT	GCTGGTTGTAGGGGATGTCT
ALDH6A1	GAACTGCCATCTTCACCACC	TGGATGCCCTGTTTGCCATA
AUH	TGATATACGAGTAGCAGCTTCCT	CCCTCCTGGTTCTGTTCCA
B2M	TGTCTTTCAGCAAGGACTGG	AGCAAGCAAGCAGAATTTGG
BCAT2	CGCTCCTGTTCGTCATTCTC	CTAACACGGTGGGCCCATA
BCKDHB	GAGAGGTAGCTTCCATGGCA	TGATTTCCGATGCAAAGCCG
BCKDK	TAACGCCCACCATGATGCT	GCCTGGTCCTTGATCGGA
DBT	AAAACAACTGCTGCTCTCCG	TGCTATCAAACTGAGACACTGT
DLD	TGGTGCAGGAGTAATAGGTGT	GCTTTACCACCAGAAGCAGC
ESRRA	ACTATGGTGTGGCATCCTGT	CCGGACAGCTGTACTCGAT
HIBADH	AGCAGTTTTCATGGATGCCC	AACAGCTCCACAGTACACCA
IVD	CACTTCCAGTTGATGCAGGG	AAACACTGAATGCCGTCCAG
GUSB	CAGAGCGAGTATGGAGCAGA	ACTCTCGTCGGTGACTGTTC
MCCC1	GGGAGACTGCACTTACCTGA	TCCAGCTTTGACAAACACCTT
MCCC2	GGAGGTGGCATTATTACAGGC	TGCTCCTCCCGAATCAACTA
MUT	GCCCTCTTTTCCAGACTCCT	GGTATCACCCCTCCACACAT
PCCA	TGATGAAGAGACCAGGGATGG	TCGAGTCTCCGCATCCAAAA
PCCB	CGATCCCAGTGACCGTCTG	TCCAACAGTCCTCCCATTCA
PPARGC1A	TCTGAGTCTGTATGGAGTGACAT	CCAAGTCGTTCACATCTAGTTCA
PPM1K	AAGCCTTTTCGAGTCATGCC	GCTGCCCCAAACTATTCCAA
TBP	AACAACAGCCTGCCACCTTA	GCCATAAGGCATCATTGGAC
TFAM	CTGTCTTGGCAAGTTGTCCA	CAACGCTGGGCAATTCTTCT
VEGFA	CAGAAGGAGGAGGGCAGAAT	CATCAGGGGCACACAGGAT

Table S2. Forward and reverse sequences of primers used in gene expression analysis of mouse skeletal muscle.

Gene	Forward sequence (5' to 3')	Reverse sequence (5' to 3')
ACAD8	GGCTACGGCTATCTGAAGGA	CCTGAAGCAGGTTTCGAGAG
ACADM	GCCCAGAGAGCTCTAGACGA	GTTCAACCTTCATCGCCATT
ACADSB	AAGCCTTGCGAGCTTAACAG	TCCAAGGAGACAAGCAGGTT
ALDH6A1	CTTCTGGATGGGCGAAGAAT	TGTTTCTGTCTCCAAAACCACA
AUH	GCAATTAACCAAGGGATGGA	AGCGAGGAGGTCTTTTCTCC
B2M	TTCTGGTGCTTGTCTCACTGA	CAGTATGTTCGGCTTCCCATTC
BCAT2	TACGTCATTCTGTGCCCTGT	CCTCTCTTCTGGGCTTCTCG
BCKDHA	GGCCGGATCTCCTTCTACAT	TAGTCCCGGTACATGAGCAC
BCKDHB	GGTAATACCCCGAAGCCCTT	AGGGTTCTACTGGGACCTGT
BCKDK	GCTACATGAAGACAAGCCTGA	GCATGGGAATGAAGGGGAAC
DBT	CGCGTGGAATCAAACTCTCC	CCCAATGTTGTGAGAAGCCTT
DLD	GGCATGGTGAAGATTCTTGG	GAAGCACCATATTCCAATGC
HIBADH	GGGAGCTGTTTTCATGGACG	CATTCCAGCAACTCTTGGGC
IVD	TCGATATTGCCTGTGGACGA	GGGGCCAGGTTCTCTTGAA
MCCC1	TCCAGTGAGTGCAGAAGGAG	ACCATCAGAGAGTCTCCAGC
MCCC2	CAACTTACCTCGGCAAGCAG	GTACAGGAGCCCATGACCAC
PCCA	GCATCCAGTTTCTTGGCACA	TCTGCTACCATGTCTCCAGG
PCCB	TCCTGAGCTGGACACAGTTG	TTTTTGCGTAACTGGGCATT
PPARGC1A	TATGGAGTGACATAGAGTGTGCT	CCACTTCAATCCACCCAGAAAG
PPM1K	ACAAGGATTAAGCTCTACCATGC	GTGCTGTTGTCTTCGGTACC
RPLP0	AGATTCGGGATATGCTGTTGGC	TCGGGTCCTAGACCAGTGTTC
TBP	CCTTGTACCCTTCACCAATGAC	ACAGCCAAGATTCACGGTAGA

REFERENCES

Al-Khalili, L., Chibalin, A.V., Kannisto, K., Zhang, B.B., Permert, J., Holman, G.D., Ehrenborg, E., Ding, V.D., Zierath, J.R., and Krook, A. (2003). Insulin action in cultured human skeletal muscle cells during differentiation: assessment of cell surface GLUT4 and GLUT1 content. Cell Mol Life Sci *60*, 991-998.

Batista, T.M., Garcia-Martin, R., Cai, W., Konishi, M., O'Neill, B.T., Sakaguchi, M., Kim, J.H., Jung, D.Y., Kim, J.K., and Kahn, C.R. (2019). Multi-dimensional transcriptional remodeling by physiological insulin in vivo. Cell Rep *26*, 3429-3443 e3423.

Chorell, E., Ryberg, M., Larsson, C., Sandberg, S., Mellberg, C., Lindahl, B., Antti, H., and Olsson, T. (2016). Plasma metabolomic response to postmenopausal weight loss induced by different diets. Metabolomics *12*, 1-14.

Dufour, C.R., Wilson, B.J., Huss, J.M., Kelly, D.P., Alaynick, W.A., Downes, M., Evans, R.M., Blanchette, M., and Giguere, V. (2007). Genome-wide orchestration of cardiac functions by the orphan nuclear receptors ERRalpha and gamma. Cell Metab *5*, 345-356.

Estall, J.L., Kahn, M., Cooper, M.P., Fisher, F.M., Wu, M.K., Laznik, D., Qu, L., Cohen, D.E., Shulman, G.I., and Spiegelman, B.M. (2009). Sensitivity of lipid metabolism and insulin signaling to genetic alterations in hepatic peroxisome proliferator-activated receptor-gamma coactivator-1alpha expression. Diabetes *58*, 1499-1508.

Evans, A.M., DeHaven, C.D., Barrett, T., Mitchell, M., and Milgram, E. (2009). Integrated, nontargeted ultrahigh performance liquid chromatography/electrospray ionization tandem mass spectrometry platform for the identification and relative quantification of the small-molecule complement of biological systems. Anal Chem *81*, 6656-6667.

Felig, P., Marliss, E., and Cahill, G.F., Jr. (1969). Plasma amino acid levels and insulin secretion in obesity. N Engl J Med *281*, 811-816.

Fukagawa, N.K., Minaker, K.L., Rowe, J.W., Goodman, M.N., Matthews, D.E., Bier, D.M., and Young, V.R. (1985). Insulin-mediated reduction of whole body protein breakdown. Dose-response effects on leucine metabolism in postabsorptive men. J Clin Invest *76*, 2306-2311.

Galgani, J.E., Moro, C., and Ravussin, E. (2008). Metabolic flexibility and insulin resistance. Am J Physiol Endocrinol Metab *295*, E1009-1017.

Hagg, S.A., Morse, E.L., and Adibi, S.A. (1982). Effect of exercise on rates of oxidation, turnover, and plasma clearance of leucine in human subjects. Am J Physiol *242*, E407-410.

Handschin, C., Chin, S., Li, P., Liu, F., Maratos-Flier, E., Lebrasseur, N.K., Yan, Z., and Spiegelman, B.M. (2007). Skeletal muscle fiber-type switching, exercise intolerance, and myopathy in PGC-1alpha muscle-specific knock-out animals. J Biol Chem *282*, 30014-30021.

Hatazawa, Y., Minami, K., Yoshimura, R., Onishi, T., Manio, M.C., Inoue, K., Sawada, N., Suzuki, O., Miura, S., and Kamei, Y. (2016). Deletion of the transcriptional coactivator PGC1alpha in skeletal muscles is associated with reduced expression of genes related to oxidative muscle function. Biochem Biophys Res Commun *481*, 251-258.

Hatazawa, Y., Tadaishi, M., Nagaike, Y., Morita, A., Ogawa, Y., Ezaki, O., Takai-Igarashi, T., Kitaura, Y., Shimomura, Y., Kamei, Y., et al. (2014). PGC-1alpha-mediated branched-chain amino acid metabolism in the skeletal muscle. PLoS One *9*, e91006.

Herman, M.A., She, P., Peroni, O.D., Lynch, C.J., and Kahn, B.B. (2010). Adipose tissue branched chain amino acid (BCAA) metabolism modulates circulating BCAA levels. J Biol Chem *285*, 11348-11356.

Ho, J.E., Larson, M.G., Vasan, R.S., Ghorbani, A., Cheng, S., Rhee, E.P., Florez, J.C., Clish, C.B., Gerszten, R.E., and Wang, T.J. (2013). Metabolite profiles during oral glucose challenge. Diabetes *62*, 2689-2698.

Huffman, K.M., Shah, S.H., Stevens, R.D., Bain, J.R., Muehlbauer, M., Slentz, C.A., Tanner, C.J., Kuchibhatla, M., Houmard, J.A., Newgard, C.B., et al. (2009). Relationships between circulating metabolic intermediates and insulin action in overweight to obese, inactive men and women. Diabetes Care *32*, 1678-1683.

Huss, J.M., Torra, I.P., Staels, B., Giguere, V., and Kelly, D.P. (2004). Estrogen-related receptor alpha directs peroxisome proliferator-activated receptor alpha signaling in the transcriptional control of energy metabolism in cardiac and skeletal muscle. Mol Cell Biol *24*, 9079-9091.

Jang, C., Oh, S.F., Wada, S., Rowe, G.C., Liu, L., Chan, M.C., Rhee, J., Hoshino, A., Kim, B., Ibrahim, A., et al. (2016). A branched-chain amino acid metabolite drives vascular fatty acid transport and causes insulin resistance. Nat Med *22*, 421-426.

Leahy, J.L. (2005). Pathogenesis of type 2 diabetes mellitus. Arch Med Res *36*, 197-209.

Lerin, C., Goldfine, A.B., Boes, T., Liu, M., Kasif, S., Dreyfuss, J.M., De Sousa-Coelho, A.L., Daher, G., Manoli, I., Sysol, J.R., et al. (2016). Defects in muscle branched-chain amino acid oxidation contribute to impaired lipid metabolism. Molecular metabolism *5*, 926-936.

Lin, J., Wu, H., Tarr, P.T., Zhang, C.Y., Wu, Z., Boss, O., Michael, L.F., Puigserver, P., Isotani, E., Olson, E.N., et al. (2002). Transcriptional co-activator PGC-1 alpha drives the formation of slow-twitch muscle fibres. Nature *418*, 797-801.

Lin, J., Wu, P.H., Tarr, P.T., Lindenberg, K.S., St-Pierre, J., Zhang, C.Y., Mootha, V.K., Jager, S., Vianna, C.R., Reznick, R.M., et al. (2004). Defects in adaptive energy metabolism with CNS-linked hyperactivity in PGC-1alpha null mice. Cell *119*, 121-135.

Lotta, L.A., Scott, R.A., Sharp, S.J., Burgess, S., Luan, J., Tillin, T., Schmidt, A.F., Imamura, F., Stewart, I.D., Perry, J.R., et al. (2016). Genetic Predisposition to an Impaired Metabolism of the Branched-Chain Amino Acids and Risk of Type 2 Diabetes: A Mendelian Randomisation Analysis. PLoS medicine *13*, e1002179.

Luo, J., Sladek, R., Carrier, J., Bader, J.A., Richard, D., and Giguere, V. (2003). Reduced fat mass in mice lacking orphan nuclear receptor estrogen-related receptor alpha. Mol Cell Biol *23*, 7947-7956.

Menni, C., Fauman, E., Erte, I., Perry, J.R., Kastenmuller, G., Shin, S.Y., Petersen, A.K., Hyde, C., Psatha, M., Ward, K.J., et al. (2013). Biomarkers for type 2 diabetes and impaired fasting glucose using a nontargeted metabolomics approach. Diabetes *62*, 4270-4276.

Mootha, V.K., Handschin, C., Arlow, D., Xie, X., St Pierre, J., Sihag, S., Yang, W., Altshuler, D., Puigserver, P., Patterson, N., et al. (2004). Erralpha and Gabpa/b specify PGC-1alpha-dependent oxidative phosphorylation gene expression that is altered in diabetic muscle. Proc Natl Acad Sci U S A *101*, 6570-6575.

Moreno-Santos, I., Perez-Belmonte, L.M., Macias-Gonzalez, M., Mataro, M.J., Castellano, D., Lopez-Garrido, M., Porras-Martin, C., Sanchez-Fernandez, P.L., Gomez-Doblas, J.J., Cardona, F., et al. (2016). Type 2 diabetes is associated with decreased PGC1alpha expression in epicardial adipose tissue of patients with coronary artery disease. J Transl Med *14*, 243.

Neinast, M.D., Jang, C., Hui, S., Murashige, D.S., Chu, Q., Morscher, R.J., Li, X., Zhan, L., White, E., Anthony, T.G., et al. (2019). Quantitative analysis of the whole-body metabolic fate of branched-chain amino acids. Cell Metab *29*, 417-429 e414.

Newgard, C.B., An, J., Bain, J.R., Muehlbauer, M.J., Stevens, R.D., Lien, L.F., Haqq, A.M., Shah, S.H., Arlotto, M., Slentz, C.A., et al. (2009). A branched-chain amino acid-related metabolic signature that differentiates obese and lean humans and contributes to insulin resistance. Cell Metab *9*, 311-326.

Nie, C., He, T., Zhang, W., Zhang, G., and Ma, X. (2018). Branched chain amino acids: Beyond nutrition metabolism. Int J Mol Sci *19*, 954.

Patti, M.E., Brambilla, E., Luzi, L., Landaker, E.J., and Kahn, C.R. (1998). Bidirectional modulation of insulin action by amino acids. J Clin Invest *101*, 1519-1529.

Patti, M.E., Butte, A.J., Crunkhorn, S., Cusi, K., Berria, R., Kashyap, S., Miyazaki, Y., Kohane, I., Costello, M., Saccone, R., et al. (2003). Coordinated reduction of genes of oxidative metabolism in humans with insulin resistance and diabetes: Potential role of PGC1 and NRF1. Proc Natl Acad Sci U S A *100*, 8466-8471.

Puigserver, P., and Spiegelman, B.M. (2003). Peroxisome proliferator-activated receptor-gamma coactivator 1 alpha (PGC-1 alpha): transcriptional coactivator and metabolic regulator. Endocr Rev *24*, 78-90.

Schooneman, M.G., Vaz, F.M., Houten, S.M., and Soeters, M.R. (2013). Acylcarnitines: reflecting or inflicting insulin resistance? Diabetes *62*, 1-8.

Schreiber, S.N., Emter, R., Hock, M.B., Knutti, D., Cardenas, J., Podvinec, M., Oakeley, E.J., and Kralli, A. (2004). The estrogen-related receptor alpha (ERRalpha) functions in PPARgamma coactivator 1alpha (PGC-1alpha)-induced mitochondrial biogenesis. Proc Natl Acad Sci U S A *101*, 6472-6477.

Shah, S.H., Crosslin, D.R., Haynes, C.S., Nelson, S., Turer, C.B., Stevens, R.D., Muehlbauer, M.J., Wenner, B.R., Bain, J.R., Laferrere, B., et al. (2012). Branched-chain amino acid levels are associated with improvement in insulin resistance with weight loss. Diabetologia *55*, 321-330.

Shaham, O., Wei, R., Wang, T.J., Ricciardi, C., Lewis, G.D., Vasan, R.S., Carr, S.A., Thadhani, R., Gerszten, R.E., and Mootha, V.K. (2008). Metabolic profiling of the human response to a glucose challenge reveals distinct axes of insulin sensitivity. Mol Syst Biol *4*, 214.

Shin, A.C., Fasshauer, M., Filatova, N., Grundell, L.A., Zielinski, E., Zhou, J.Y., Scherer, T., Lindtner, C., White, P.J., Lapworth, A.L., et al. (2014). Brain insulin lowers circulating BCAA levels by inducing hepatic BCAA catabolism. Cell Metab *20*, 898-909.

Staron, R.S., Hagerman, F.C., Hikida, R.S., Murray, T.F., Hostler, D.P., Crill, M.T., Ragg, K.E., and Toma, K. (2000). Fiber type composition of the vastus lateralis muscle of young men and women. J Histochem Cytochem *48*, 623-629.

Suhre, K., Meisinger, C., Doring, A., Altmaier, E., Belcredi, P., Gieger, C., Chang, D., Milburn, M.V., Gall, W.E., Weinberger, K.M., et al. (2010). Metabolic footprint of diabetes: a multiplatform metabolomics study in an epidemiological setting. PLoS One *5*, e13953.

Svensson, K., Albert, V., Cardel, B., Salatino, S., and Handschin, C. (2016). Skeletal muscle PGC-1alpha modulates systemic ketone body homeostasis and ameliorates diabetic hyperketonemia in mice. FASEB J *30*, 1976-1986.

Tessari, P., Trevisan, R., Inchiostro, S., Biolo, G., Nosadini, R., De Kreutzenberg, S.V., Duner, E., Tiengo, A., and Crepaldi, G. (1986). Dose-response curves of effects of insulin on leucine kinetics in humans. Am J Physiol *251*, E334-342.

van Doorn, M., Vogels, J., Tas, A., van Hoogdalem, E.J., Burggraaf, J., Cohen, A., and van der Greef, J. (2007). Evaluation of metabolite profiles as biomarkers for the pharmacological effects of thiazolidinediones in Type 2 diabetes mellitus patients and healthy volunteers. Br J Clin Pharmacol *63*, 562-574.

Wu, Z., Puigserver, P., Andersson, U., Zhang, C., Adelmant, G., Mootha, V., Troy, A., Cinti, S., Lowell, B., Scarpulla, R.C., et al. (1999). Mechanisms controlling mitochondrial biogenesis and respiration through the thermogenic coactivator PGC-1. Cell *98*, 115-124.

Wurtz, P., Soininen, P., Kangas, A.J., Ronnemaa, T., Lehtimaki, T., Kahonen, M., Viikari, J.S., Raitakari, O.T., and Ala-Korpela, M. (2013). Branched-chain and aromatic amino acids are predictors of insulin resistance in young adults. Diabetes Care *36*, 648-655.

Xu, F., Tavintharan, S., Sum, C.F., Woon, K., Lim, S.C., and Ong, C.N. (2013). Metabolic signature shift in type 2 diabetes mellitus revealed by mass spectrometry-based metabolomics. J Clin Endocrinol Metab *98*, E1060-1065.

Yoon, J.C., Puigserver, P., Chen, G., Donovan, J., Wu, Z., Rhee, J., Adelmant, G., Stafford, J., Kahn, C.R., Granner, D.K., et al. (2001). Control of hepatic gluconeogenesis through the transcriptional coactivator PGC-1. Nature *413*, 131-138.

Yu, D., Moore, S.C., Matthews, C.E., Xiang, Y.B., Zhang, X., Gao, Y.T., Zheng, W., and Shu, X.O. (2016). Plasma metabolomic profiles in association with type 2 diabetes risk and prevalence in Chinese adults. Metabolomics *12*.

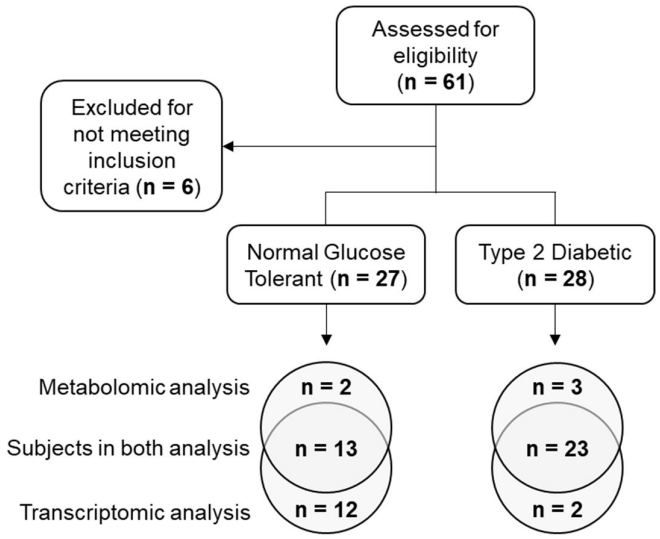
Assessed for eligibility (n = 61)
Excluded for not meeting inclusion criteria (n = 6)
Normal Glucose Tolerant (n = 27)
Type 2 Diabetic (n = 28)
Metabolomic analysis
Subjects in both analysis
Transcriptomic analysis
n = 2
n = 13
n = 12
n = 3
n = 23
n = 2

Figure 1.

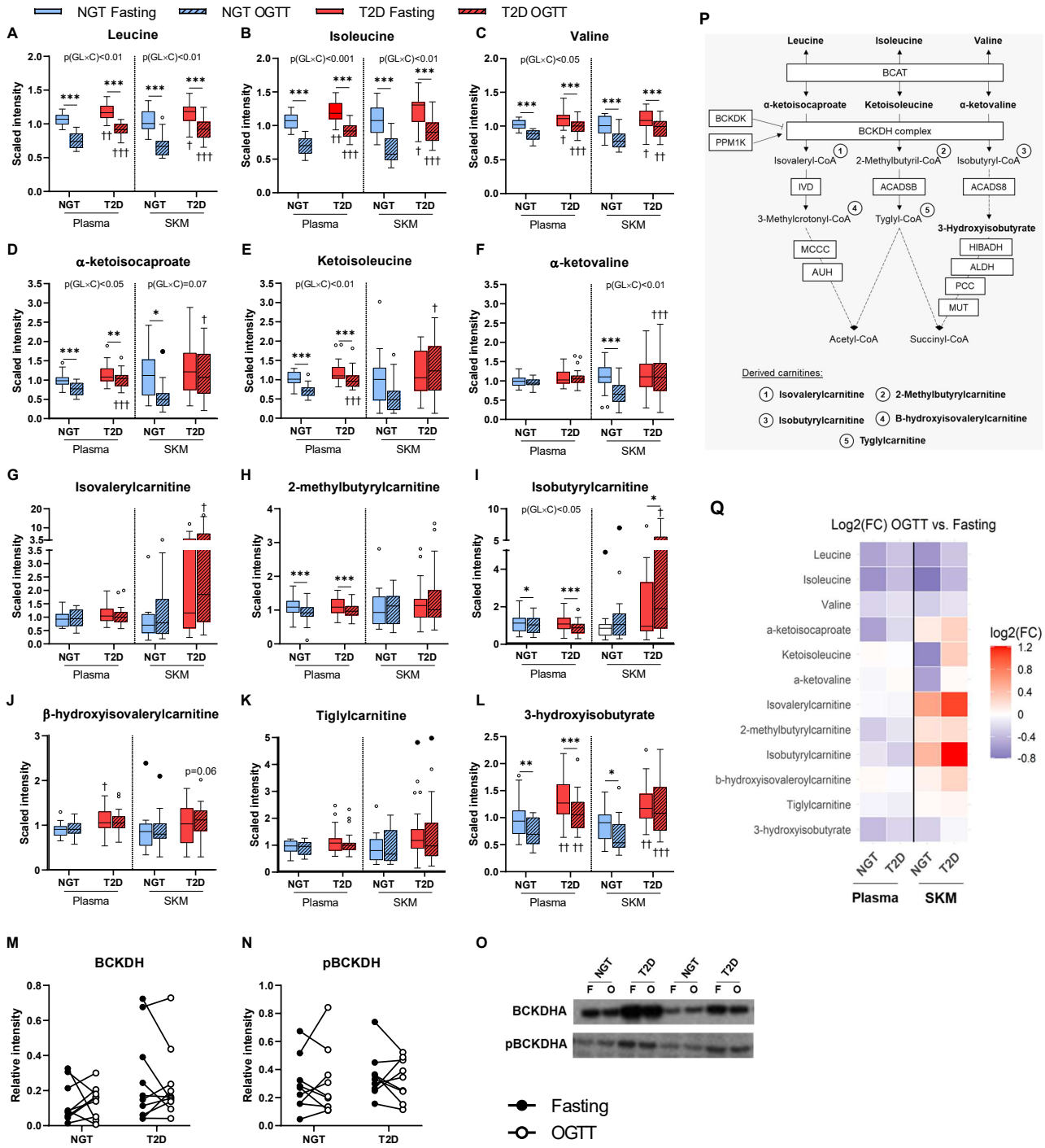
NGT Fasting
NGT OGTT
T2D Fasting
T2D OGTT
A
Leucine
B
Isoleucine
C
Valine
D
α-ketoisocaproate
E
Ketoisoleucine
F
α-ketovaline
G
Isovalerylcarnitine
H
2-methylbutyrylcarnitine
I
Isobutyrylcarnitine
J
β-hydroxyisovalerylcarnitine
K
Tiglylcarnitine
L
3-hydroxyisobutyrate
Scaled intensity
Plasma
SKM
NGT
T2D
M
BCKDH
N
pBCKDH
Relative intensity
O
BCKDHA
pBCKDHA
Fasting
OGTT
P
Leucine
Isoleucine
Valine
BCAT
α-ketoisocaproate
Ketoisoleucine
α-ketovaline
BCKDK
PPM1K
BCKDH complex
Isovaleryl-CoA
2-Methylbutyril-CoA
Isobutyryl-CoA
IVD
ACADSB
ACADS8
3-Methylcrotonyl-CoA
Tyglyl-CoA
3-Hydroxyisobutyrate
MCCC
AUH
HIBADH
ALDH
PCC
MUT
Acetyl-CoA
Succinyl-CoA
Derived carnitines:
1 Isovalerylcarnitine
2 2-Methylbutyrylcarnitine
3 Isobutyrylcarnitine
4 B-hydroxyisovalerylcarnitine
5 Tyglylcarnitine
Q
Log2(FC) OGTT vs. Fasting
Leucine
Isoleucine
Valine
a-ketoisocaproate
Ketoisoleucine
a-ketovaline
Isovalerylcarnitine
2-methylbutyrylcarnitine
Isobutyrylcarnitine
b-hydroxyisovaleroylcarnitine
Tiglylcarnitine
3-hydroxyisobutyrate
log2(FC)
Plasma
SKM

Figure 2.

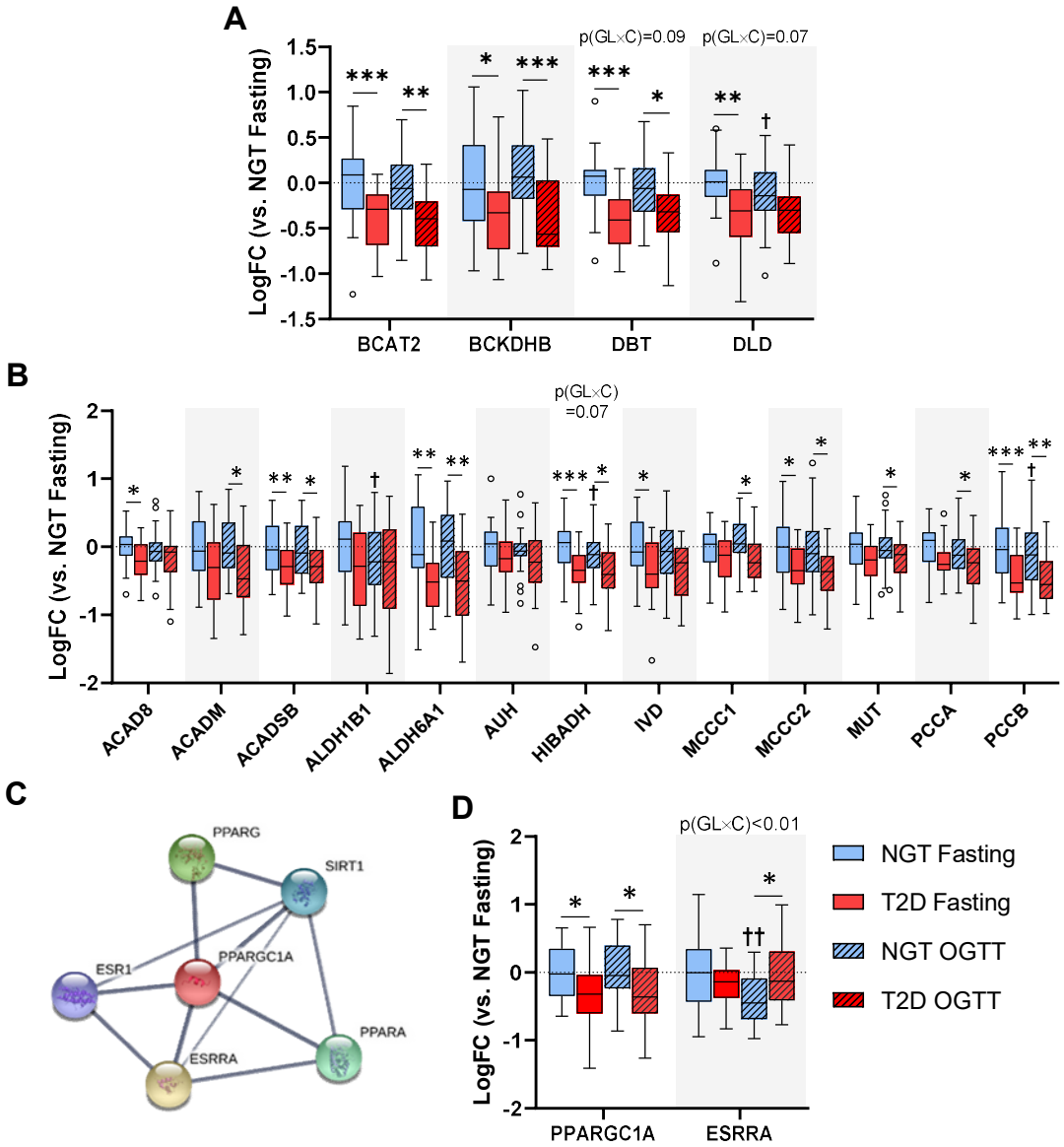
A
LogFC (vs. NGT Fasting)
p(GL×C)=0.09
p(GL×C)=0.07
BCAT2
BCKDHB
DBT
DLD
B
LogFC (vs. NGT Fasting)
p(GL×C)
=0.07
ACAD8
ACADM
ACADSB
ALDH1B1
ALDH6A1
AUH
HIBADH
IVD
MCCC1
MCCC2
MUT
PCCA
PCCB
C
PPARG
SIRT1
ESR1
PPARGC1A
PPARA
ESRRA
D
LogFC (vs. NGT Fasting)
p(GL×C)<0.01
PPARGC1A
ESRRA
NGT Fasting
T2D Fasting
NGT OGTT
T2D OGTT

Figure 3.

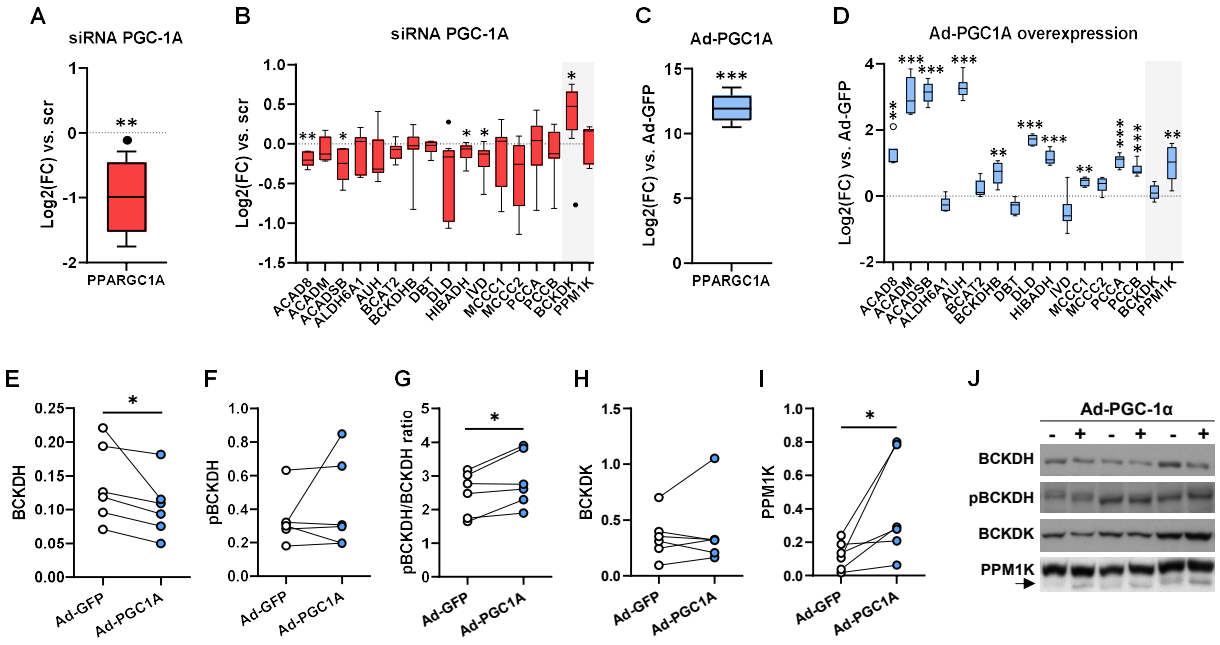
A
siRNA PGC-1A
Log2(FC) vs. scr
PPARGC1A
B
siRNA PGC-1A
Log2(FC) vs. scr
ACAD8
ACADM
ACADSB
ALDH6A1
AUH
BCAT2
BCKDHB
DBT
DLD
HIBADH
IVD
MCCC1
MCCC2
PCCA
PCCB
BCKDK
PPM1K
C
Ad-PGC1A
Log2(FC) vs. Ad-GFP
PPARGC1A
D
Ad-PGC1A overexpression
Log2(FC) vs. Ad-GFP
E
BCKDH
Ad-GFP
Ad-PGC1A
F
pBCKDH
G
pBCKDH/BCKDH ratio
H
BCKDK
I
PPM1K
J
Ad-PGC-1α
BCKDH
pBCKDH
BCKDK
PPM1K

Figure 4.

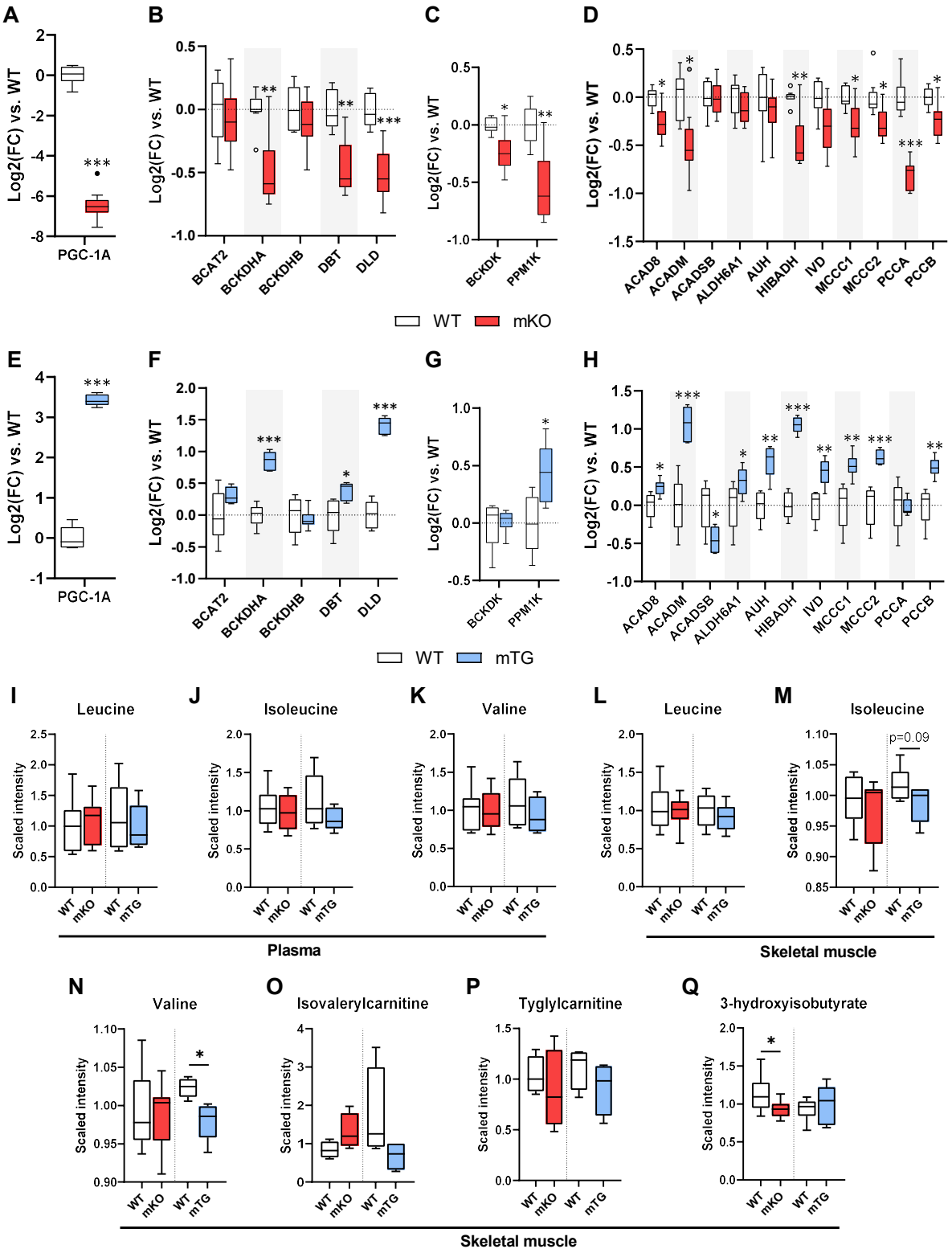
A
B
C
D
E
F
G
H
I
J
K
L
M
N
O
P
Q
Log2(FC) vs. WT
PGC-1A
BCAT2
BCKDHA
BCKDHB
DBT
DLD
BCKDK
PPM1K
ACAD8
ACADM
ACADSB
ALDH6A1
AUH
HIBADH
IVD
MCCC1
MCCC2
PCCA
PCCB
WT
mKO
mTG
Leucine
Isoleucine
Valine
Scaled intensity
p=0.09
Plasma
Skeletal muscle
Isovalerylcarnitine
Tyglylcarnitine
3-hydroxyisobutyrate

Figure 5.

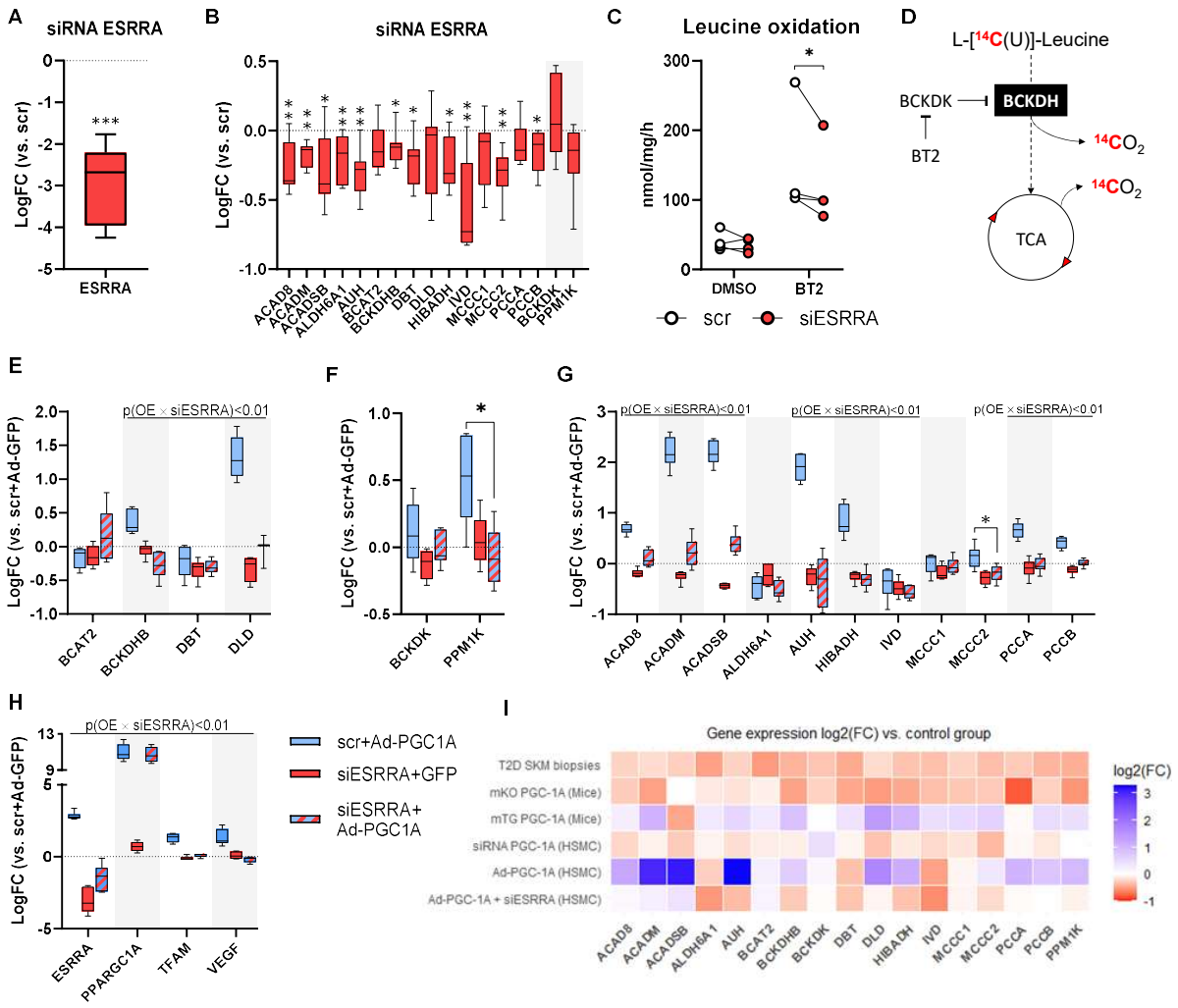
A
siRNA ESRRA
LogFC (vs. scr)
ESRRA
B
siRNA ESRRA
LogFC (vs. scr)
ACAD8
ACADM
ACADSB
ALDH6A1
AUH
BCAT2
BCKDHB
DBT
DLD
HIBADH
IVD
MCCC1
MCCC2
PCCA
PCCB
BCKDK
PPM1K
C
Leucine oxidation
nmol/mg/h
DMSO
BT2
scr
siESRRA
D
L-[14C(U)]-Leucine
BCKDK
BCKDH
BT2
14CO2
14CO2
TCA
E
p(OE × siESRRA)<0.01
LogFC (vs. scr+Ad-GFP)
BCAT2
BCKDHB
DBT
DLD
F
LogFC (vs. scr+Ad-GFP)
BCKDK
PPM1K
G
p(OE × siESRRA)<0.01
p(OE × siESRRA)<0.01
p(OE × siESRRA)<0.01
LogFC (vs. scr+Ad-GFP)
ACAD8
ACADM
ACADSB
ALDH6A1
AUH
HIBADH
IVD
MCCC1
MCCC2
PCCA
PCCB
H
p(OE × siESRRA)<0.01
LogFC (vs. scr+Ad-GFP)
ESRRA
PPARGC1A
TFAM
VEGF
scr+Ad-PGC1A
siESRRA+GFP
siESRRA+
Ad-PGC1A
I
Gene expression log2(FC) vs. control group
T2D SKM biopsies
mKO PGC-1A (Mice)
mTG PGC-1A (Mice)
siRNA PGC-1A (HSMC)
Ad-PGC-1A (HSMC)
Ad-PGC-1A + siESRRA (HSMC)
log2(FC)
ACAD8
ACADM
ACADSB
ALDH6A1
AUH
BCAT2
BCKDHB
BCKDK
DBT
DLD
HIBADH
IVD
MCCC1
MCCC2
PCCA
PCCB
PPM1K

Figure 6.